

# Exploring Ultra Rapid Data Assimilation Based on Ensemble Transform Kalman Filter with the Lorenz 96 Model

Fumitoshi Kawasaki<sup>1</sup>, Atsushi Okazaki<sup>2,3</sup>, Kenta Kurosawa<sup>2</sup>, and Shunji Kotsuki<sup>2,3,4</sup>

<sup>1</sup>Graduate School of Science and Engineering, Chiba University, Chiba, Japan

<sup>2</sup>Center for Environmental Remote Sensing, Chiba University, Chiba, Japan

<sup>3</sup>Institute for Advanced Academic Research, Chiba University, Chiba, Japan

<sup>4</sup>Research Institute of Disaster Medicine, Chiba University, Chiba, Japan

**Correspondence:** Fumitoshi Kawasaki, Graduate School of Science and Engineering, Chiba University, 1-33, Yayoicho, Inage-ku, Chiba-shi, Chiba, 263-8522, Japan.

**Email:** fkawasaki@chiba-u.jp

## Abstract

To explore the effectiveness of ultra-rapid data assimilation (URDA) for numerical weather prediction (NWP), this study investigates the properties of URDA in nonlinear models and proposes technical treatments to enhance its performance. URDA rapidly updates preemptive forecasts derived from observations without integrating a dynamical model each time additional observations become available. First, we analytically demonstrate that the preemptive forecast obtained by URDA in nonlinear models is approximately equivalent to the forecast integrated from the analysis. Furthermore, numerical experiments are conducted with the 40-variable Lorenz 96 model. The results show that URDA in nonlinear models tends to exhibit deterioration of forecast accuracy and collapse of ensemble spread when preemptive forecasts are repeatedly updated or when the forecasts are extended over longer periods. Furthermore, the roles of inflation and localization, both essential technical treatments in NWP, are examined in the context of URDA. It is shown that although inflation and localization are essential to URDA, conventional inflation techniques are not suitable for it. Therefore, this study proposes new technical treatments for URDA, namely relaxation to baseline perturbations (RTBP) and relaxation to baseline forecast (RTBF). Applying RTBP and RTBF mitigates the difficulties associated with URDA and yields preemptive forecasts with higher accuracy than the baseline forecast. Consequently, URDA, particularly when combined with RTBP and RTBF, would stand as a step toward practical application in NWP.

## 1 INTRODUCTION

The forecasting performance of numerical weather prediction (NWP) has improved significantly over the past few decades due to advances in NWP models, observational techniques, data assimilation methods, and computational technologies (Bauer et al., 2015; Evensen et al., 2022; Kalnay, 2002). However, NWP still faces challenges and limitations. One such issue is that the assimilation and forecast cycles are constrained to several hours in many global and regional models due mainly to the huge computational costs of the data assimilation process and the model forecast process (Etherton, 2007; Madaus and Hakim, 2015; Potthast and Welzbacher, 2018; Zhang et al., 2023). In addition, four-dimensional data assimilation, which is employed by many operational NWP centers, requires extending the data assimilation window to incorporate many observations. This requirement may also limit high-frequency assimilation and forecast cycles. For example, in the mesoscale ensemble prediction system (MEPS) of the Japan Meteorological Agency (JMA), the frequency of 39-hour forecasts is restricted to every 6 hours. Additionally, in the medium-range ensemble forecast system (ENS) of the European Centre for Medium-Range Weather Forecasts (ECMWF), the frequency is limited to 12-hour intervals for 15-day forecasts, and to 6-hour intervals when 6-day forecasts are included.

Such infrequent assimilation and forecast cycles pose difficulties for proper decision-making in fields requiring immediacy, such as disaster prevention, aviation, and transportation. These fields require accurate prediction of rapidly evolving meteorological phenomena, including torrential rainfall associated with convection and localized squalls. However, since such meteorological phenomena occur on short time scales, significant discrepancies can arise between forecasts and actual weather conditions when assimilation and forecast cycles span several hours. If more frequent assimilation and forecast cycles were realized, the timeliness and accuracy of forecasts would be improved, thereby enhancing the reliability of action plans and preventive measures. As a result, the operational value of NWP in these fields would be further increased.

To address such issues, approaches that update forecasts rapidly without integrating dynamical models each time additional observations become available have been explored. First, Etherton (2007) proposed a concept termed the preemptive forecast. The basis of this concept is to update the forecast by propagating the analysis increment obtained from data assimilation into the future and adding it to the mean of the existing forecast ensemble. That is, since this forecast update does not require integrating dynamical models, the computational cost is essentially only for the data assimilation process. Therefore, the computational costs of the preemptive forecast are much lower than those of the assimilation and forecast cycles (Etherton, 2007). Note that, for the preemptive forecast, it is assumed that ensemble Kalman filter (EnKF; Evensen, 1994) is used rather than variational methods such as four-dimensional variational data assimilation (4DVar; Dimet and Talagrand, 1986; Talagrand and Courtier, 1987) and ensemble variational data assimilation (EnVAR; Liu et al., 2008). Therefore, to be precise, the computational cost required for the preemptive forecast corresponds to that of EnKF, which is generally less expensive than the variational methods. Etherton (2007) showed that the accuracy of preemptive forecasts updated based on the latest observations improved compared to the baseline 24-hour or 48-hour forecasts, using the barotropic vorticity model. Subsequently, Madaus and Hakim (2015) extended the preemptive forecast concept by proposing the ensemble forecast adjustment (EFA). EFA implements a preemptive forecast through the serial ensemble square root filter (serial EnSRF; Whitaker and Hamill, 2002), updating not only the ensemble forecast mean but also the ensemble forecast perturbations. Madaus and Hakim (2015) conducted their experiments using operational ensemble forecasts of the ECMWF and the Canadian Meteorological Centre (CMC). As a result, the preemptive forecasts of surface pressure obtained from an additional surface pressure observation showed improved accuracy up to 24 hours after the observation time in both operational centers. Furthermore, Potthast and Welzbacher (2018) proposed ultra-rapid data assimilation (URDA) based on these studies. URDA can be essentially regarded as an implementation of a preemptive forecast using the ensemble transform Kalman filter (ETKF; Bishop et al., 2001). The formulation of URDA with the product of ensemble transform matrices (cf. Section 2.3) explicitly emphasizes updating preemptive forecasts sequentially with multiple observations. Potthast and Welzbacher (2018) analytically proved that the preemptive forecast with URDA is identical to the forecast from the analysis ensemble of EnKF when the system and the observation operator are linear. Furthermore, Potthast and Welzbacher (2018) demonstrated that URDA is effective even in nonlinear models by conducting experiments using the Lorenz 63 model (Lorenz, 1963).

Toward practical applications of URDA in NWP, this study investigates its properties in nonlinear models and proposes technical treatments to improve its performance. Specifically, in nonlinear models, we first demonstrate analytically that the preemptive forecast of URDA is approximately equivalent to the forecast derived from the analysis of EnKF. Although Potthast and Welzbacher (2018) numerically showed that URDA yields promising results even for nonlinear models through experiments using the Lorenz 63 model, our proof provides an analytical explanation for why URDA is effective in nonlinear models. In addition, in NWP, technical treatments such as inflation and localization are indispensable for stable and efficient data assimilation. Therefore, this study investigates the influence of inflation and localization. For this purpose, this study implements URDA using the local ensemble transform Kalman filter (LETKF; Hunt et al., 2007). Furthermore, in nonlinear models, we discuss the tendency for the forecast accuracy to deteriorate and the ensemble spread to collapse sharply when preemptive forecasts are repeatedly updated or when forecasts are extended over long periods. To address this difficulty, this study proposes new technical treatments for URDA

in nonlinear models, namely relaxation to baseline perturbations (RTBP) and relaxation to baseline forecast (RTBF).

If URDA can be applied to NWP based on the fundamental insights gained from this investigation, more frequent updates of the assimilation and forecast cycles may become feasible. Additionally, apart from enabling rapid forecast updates, URDA has the following advantages, giving it high potential for applications in NWP.

- By incorporating URDA within four-dimensional ensemble data assimilation systems, URDA enables high-frequency preemptive forecasts based on the latest observations while maintaining an extended data assimilation window.
- Unlike conventional forecasting frameworks, URDA does not require the full forecast state vector to be updated; instead, it allows selective updating of subsets of forecast states of interest (Madaus and Hakim, 2015; Potthast and Welzbacher, 2018).
- If the system already incorporates LETKF scheme, URDA can be implemented easily.

In this study, we conduct numerical experiments using the 40-dimensional Lorenz 96 model (Lorenz, 1996), which is known as a chaotic dynamical system. This is because the Lorenz 96 model can emphasize the effect of localization more easily than the three-dimensional Lorenz 63 model. Specifically, we first highlight the difficulties of URDA in nonlinear models. Additionally, sensitivity experiments on parameters related to inflation and localization are conducted to investigate the roles of these technical treatments in URDA. In this study, multiplicative inflation (Anderson and Anderson, 1999), relaxation to prior perturbations (RTPP; Zhang et al., 2004), and relaxation to prior spread (RTPS; Whitaker and Hamill, 2012), which have been used mainly in data assimilation studies, are employed as inflation techniques. Subsequently, we demonstrate the effectiveness of the proposed URDA by showing that the difficulties of URDA in nonlinear models are mitigated.

The remainder of this paper is organized as follows. In Section 2, we describe the methodologies, including URDA, RTBP, and RTBF. Section 3 presents the experimental design of URDA using the Lorenz 96 model. Section 4 shows the experimental results, and Section 5 presents the discussion. Finally, we provide a conclusion in Section 6.

## 2 METHODOLOGY

### 2.1 EnKF

In this section, we introduce the basic formulas of EnKF. Let the dimension of the model space be  $n \in \mathbb{N}$ , and the dimension of the ensemble space be  $m \in \mathbb{N}$ . The forecast ensemble  $\mathbf{X}^f \in \mathbb{R}^{n \times m}$ , the forecast ensemble mean  $\bar{\mathbf{x}}^f \in \mathbb{R}^n$ , and the forecast ensemble perturbation  $\delta\mathbf{X}^f \in \mathbb{R}^{n \times m}$  are defined using the forecast ensemble members  $\mathbf{x}^{f(i)} \in \mathbb{R}^n$  as follows:

$$\mathbf{X}^f := \left[ \mathbf{x}^{f(1)}, \dots, \mathbf{x}^{f(m)} \right], \quad (1)$$

$$\bar{\mathbf{x}}^f := \frac{1}{m} \sum_{i=1}^m \mathbf{x}^{f(i)}, \quad (2)$$

$$\delta\mathbf{X}^f := \left[ \mathbf{x}^{f(1)} - \bar{\mathbf{x}}^f, \dots, \mathbf{x}^{f(m)} - \bar{\mathbf{x}}^f \right]. \quad (3)$$

In addition, the analysis ensemble is defined in the same manner as the forecast ensemble:

$$\mathbf{X}^a := \left[ \mathbf{x}^{a(1)}, \dots, \mathbf{x}^{a(m)} \right], \quad (4)$$

$$\bar{\mathbf{x}}^a := \frac{1}{m} \sum_{i=1}^m \mathbf{x}^{a(i)}, \quad (5)$$

$$\delta\mathbf{X}^a := \left[ \mathbf{x}^{a(1)} - \bar{\mathbf{x}}^a, \dots, \mathbf{x}^{a(m)} - \bar{\mathbf{x}}^a \right]. \quad (6)$$

In EnKF, the error covariance matrix based on the ensemble is typically represented as follows:

$$\mathbf{P}^f := \frac{1}{m-1} \delta \mathbf{X}^f (\delta \mathbf{X}^f)^\top, \quad (7)$$

$$\mathbf{P}^a := \frac{1}{m-1} \delta \mathbf{X}^a (\delta \mathbf{X}^a)^\top. \quad (8)$$

The analysis ensemble mean  $\bar{\mathbf{x}}^a$  is updated by the forecast ensemble mean  $\bar{\mathbf{x}}^f$  as follows:

$$\bar{\mathbf{x}}^a = \bar{\mathbf{x}}^f + \mathbf{K} (\mathbf{y}^o - H(\bar{\mathbf{x}}^f)) = \bar{\mathbf{x}}^f + \mathbf{K} \mathbf{d}^{o-f}, \quad (9)$$

where  $p \in \mathbb{N}$  denotes the dimension of the observation space,  $\mathbf{y}^o \in \mathbb{R}^p$  is the observation,  $H$  is the nonlinear observation operator,  $\mathbf{d}^{o-f} := \mathbf{y}^o - H(\bar{\mathbf{x}}^f) \in \mathbb{R}^p$  is the innovation, and  $\mathbf{K} \in \mathbb{R}^{n \times p}$  is the Kalman gain.

## 2.2 LETKF

LETKF is a data assimilation method that is widely applied in many NWP studies (e.g., Miyoshi and Aranami, 2006; Miyoshi and Yamane, 2007; Szunyogh et al., 2008) due to its advantageous properties, i.e., performing parallel computations for each grid point. For simplicity, we first describe ETKF without localization, which is the basis of LETKF.

In ETKF, both error covariance matrices are expressed as follows:

$$\mathbf{P}^f = \mathbf{Z}^f (\mathbf{Z}^f)^\top = \mathbf{Z}^f \tilde{\mathbf{P}}^f (\mathbf{Z}^f)^\top, \quad (10)$$

where  $\mathbf{Z}^f \in \mathbb{R}^{n \times m}$  is the linear map from the ensemble space  $\mathbb{R}^m$  to the model space  $\mathbb{R}^n$ , defined as follows:

$$\mathbf{Z}^f := \frac{1}{\sqrt{m-1}} \delta \mathbf{X}^f. \quad (11)$$

Also,  $\tilde{\mathbf{P}}^f \in \mathbb{R}^{m \times m}$  is regarded as the forecast error covariance matrix in the ensemble space, which is identical to the identity matrix  $\mathbf{I} \in \mathbb{R}^{m \times m}$ . In the same manner, the analysis error covariance matrix  $\mathbf{P}^a$  is expressed as follows:

$$\mathbf{P}^a = \mathbf{Z}^a (\mathbf{Z}^a)^\top = \mathbf{Z}^a \tilde{\mathbf{P}}^a (\mathbf{Z}^a)^\top, \quad (12)$$

where  $\mathbf{Z}^a \in \mathbb{R}^{n \times m}$  is defined analogously to  $\mathbf{Z}^f$ , as follows:

$$\mathbf{Z}^a := \frac{1}{\sqrt{m-1}} \delta \mathbf{X}^a. \quad (13)$$

Also,  $\tilde{\mathbf{P}}^a \in \mathbb{R}^{m \times m}$  is regarded as the analysis error covariance matrix in the ensemble space and is expressed as follows:

$$\tilde{\mathbf{P}}^a = \left[ \mathbf{I} + (\mathbf{Y}^f)^\top \mathbf{R}^{-1} \mathbf{Y}^f \right]^{-1}, \quad (14)$$

where  $\mathbf{R} \in \mathbb{R}^{p \times p}$  is the observation error covariance matrix,  $\mathbf{Y}^f \in \mathbb{R}^{p \times m}$  is the linear map from the ensemble space  $\mathbb{R}^m$  to the observation space  $\mathbb{R}^p$ , defined as follows:

$$\mathbf{Y}^f := \mathbf{H} \mathbf{Z}^f \approx \frac{1}{\sqrt{m-1}} \left[ H(\mathbf{x}^{f(1)}) - \frac{1}{m} \sum_{i=1}^m H(\mathbf{x}^{f(i)}), \dots, H(\mathbf{x}^{f(m)}) - \frac{1}{m} \sum_{i=1}^m H(\mathbf{x}^{f(i)}) \right], \quad (15)$$

where  $\mathbf{H} \in \mathbb{R}^{p \times n}$  is the linear map from the model space  $\mathbb{R}^n$  to the observation space  $\mathbb{R}^p$  (i.e., a linear observation operator). For example, refer to Kotsuki et al. (2020) for further details of the relationships between each space.

Here, we consider the update of the analysis ensemble mean  $\bar{\mathbf{x}}^a$ . The Kalman gain  $\mathbf{K}$  in Equation (9) is expressed as follows:

$$\mathbf{K} = \mathbf{P}^f \mathbf{H}^\top \left[ \mathbf{H} \mathbf{P}^f \mathbf{H}^\top + \mathbf{R} \right]^{-1} = \mathbf{Z}^f (\mathbf{Y}^f)^\top \left[ \mathbf{Y}^f (\mathbf{Y}^f)^\top + \mathbf{R} \right]^{-1}. \quad (16)$$

Here, we define the vector  $\mathbf{w}$  as follows:

$$\mathbf{w} := \left( \mathbf{Y}^f \right)^\top \left[ \mathbf{Y}^f \left( \mathbf{Y}^f \right)^\top + \mathbf{R} \right]^{-1} \mathbf{d}^{o-f}. \quad (17)$$

Therefore, from Equations (9), (16), and (17), the analysis ensemble mean  $\bar{\mathbf{x}}^a$  can be expressed as follows:

$$\bar{\mathbf{x}}^a = \bar{\mathbf{x}}^f + \mathbf{Z}^f \mathbf{w}. \quad (18)$$

Subsequently, we consider the update of the analysis ensemble perturbation  $\delta \mathbf{X}^a$ . Since an error covariance matrix is a positive semidefinite matrix, from Equation (12), the analysis ensemble perturbation  $\delta \mathbf{X}^a$  can be expressed as a linear combination of the forecast ensemble perturbation  $\delta \mathbf{X}^f$  as follows:

$$\mathbf{P}^a = \left[ \mathbf{Z}^f \left( \tilde{\mathbf{P}}^a \right)^{\frac{1}{2}} \right] \left[ \mathbf{Z}^f \left( \tilde{\mathbf{P}}^a \right)^{\frac{1}{2}} \right]^\top, \quad (19)$$

$$\iff \mathbf{Z}^a = \mathbf{Z}^f \left( \tilde{\mathbf{P}}^a \right)^{\frac{1}{2}}, \quad (20)$$

$$\iff \delta \mathbf{X}^a = \delta \mathbf{X}^f \left( \tilde{\mathbf{P}}^a \right)^{\frac{1}{2}} = \delta \mathbf{X}^f \mathbf{W}, \quad \mathbf{W} := \left( \tilde{\mathbf{P}}^a \right)^{\frac{1}{2}}. \quad (21)$$

Therefore, from Equations (18) and (21), the update equation of the analysis ensemble  $\mathbf{X}^a$  is expressed by:

$$\begin{aligned} \mathbf{X}^a &= \bar{\mathbf{x}}^a \mathbf{1}^\top + \delta \mathbf{X}^a \\ &= \bar{\mathbf{x}}^f \mathbf{1}^\top + \mathbf{Z}^f (\mathbf{w} \mathbf{1}^\top + \sqrt{m-1} \mathbf{W}) \\ &= \bar{\mathbf{x}}^f \mathbf{1}^\top + \mathbf{Z}^f \widehat{\mathbf{W}}, \quad \mathbf{1} := [1, \dots, 1]^\top, \quad \widehat{\mathbf{W}} := \mathbf{w} \mathbf{1}^\top + \sqrt{m-1} \mathbf{W}. \end{aligned} \quad (22)$$

Furthermore, the analysis ensemble  $\mathbf{X}^a$  can be expressed in terms of the properties of  $\mathbf{w}$  and  $\mathbf{W}$  (e.g., Potthast and Welzbacher, 2018) as follows:

$$\mathbf{X}^a = \frac{1}{\sqrt{m-1}} \mathbf{X}^f \widehat{\mathbf{W}} = \mathbf{X}^f \widetilde{\mathbf{W}}, \quad \widetilde{\mathbf{W}} := \frac{1}{\sqrt{m-1}} \widehat{\mathbf{W}}. \quad (23)$$

Now, we consider the update equations of LETKF, which incorporates localization. In LETKF, the analysis ensemble is computed for each grid point using only observations within the localization radius as follows:

$$\begin{aligned} \mathbf{x}_g^a &= \mathbf{x}_g^f \widetilde{\mathbf{W}}^{loc} \\ &= \mathbf{x}_g^f \left[ \frac{1}{\sqrt{m-1}} (\mathbf{Y}^{f,loc})^\top \left[ \mathbf{Y}^{f,loc} (\mathbf{Y}^{f,loc})^\top + \mathbf{R}^{loc} \right]^{-1} \mathbf{d}^{o-f,loc} \mathbf{1}^\top \right. \\ &\quad \left. + \left[ \mathbf{I} + (\mathbf{Y}^{f,loc})^\top (\mathbf{R}^{loc})^{-1} \mathbf{Y}^{f,loc} \right]^{-1/2} \right], \end{aligned} \quad (24)$$

where the subscript "g" denotes the  $g$ -th grid point (i.e.,  $\mathbf{x}_g^a, \mathbf{x}_g^f \in \mathbb{R}^m$  are row vectors), and the superscript "loc" denotes that the vector or matrix is based on the observations within the localization radius around the  $g$ -th grid point. For example, refer to Hunt et al. (2007) for details of LETKF.

### 2.3 URDA

We first clarify the problem setting for URDA. As shown in Figure 1, we assume a situation in which an ensemble forecast with a dynamical model (hereafter called the baseline forecast) has already been performed from time 0 to time  $T$ , and then additional observations become available at each subsequent time step. For the sake of simplicity, we first consider URDA without localization.

As shown in Figure 1, URDA sequentially updates preemptive forecasts based on existing forecast ensembles and additional available observations. That is, unlike ordinary data assimilation, URDA does not require computing an analysis, but only updating the forecasts. In particular, when the model and the observation operator are linear, Potthast and Welzbacher (2018) demonstrated that the following equation holds:

$$\mathbf{X}_{k|j}^f = \mathbf{X}_{k|0}^f \tilde{\mathbf{W}}_1 \cdots \tilde{\mathbf{W}}_j = \mathbf{X}_{k|0}^f \tilde{\mathbf{W}}_j^{prod}, \quad \tilde{\mathbf{W}}_j^{prod} := \tilde{\mathbf{W}}_1 \cdots \tilde{\mathbf{W}}_j, \quad (25)$$

where subscript  $k \mid j$  ( $0 \leq j < T, j < k \leq T$ ) denotes that the forecast is performed from time  $j$  to time  $k$ . In this study, we refer to  $j$  as the forecast reference time and  $k$  as the forecast lead time. Equation (25) indicates that the forecast ensemble  $\mathbf{X}_{k|j}^f$  can be updated sequentially by applying the ensemble transform matrix  $\tilde{\mathbf{W}}_j$  from the right, when an observation  $\mathbf{y}_j^o$  is available at forecast reference time  $j$ . However, for nonlinear models, the effectiveness of URDA has been demonstrated only through numerical experiments by Potthast and Welzbacher (2018).

Therefore, this study analytically demonstrates that Equation (25) holds approximately even for nonlinear models. First, we provide the following lemma to apply linear approximation.

**Lemma 2.1.** *At time  $j$ , the analysis ensemble member  $\mathbf{x}_j^{a(i)}$  is represented as follows in terms of the forecast ensemble member  $\mathbf{x}_{j|j-1}^{f(i)}$ , the forecast ensemble perturbation  $\delta\mathbf{X}_{j|j-1}^f$ , and the ensemble transform matrix  $\tilde{\mathbf{W}}_j$  :*

$$\mathbf{x}_j^{a(i)} = \mathbf{x}_{j|j-1}^{f(i)} + \sum_{l=1}^m \delta\mathbf{x}_{j|j-1}^{f(l)} \omega_{j,li}, \quad (26)$$

where  $\omega_{j,li}$  is the  $l$ -th row and  $i$ -th column element of  $\Omega_j := \tilde{\mathbf{W}}_j - \mathbf{I}$ .

*Proof.* From Equation (22), the following equation holds:

$$\begin{aligned} \mathbf{X}_j^a &= \bar{\mathbf{x}}_{j|j-1}^f \mathbf{1}^\top + \mathbf{Z}_{j|j-1}^f \tilde{\mathbf{W}}_j \\ &= \bar{\mathbf{x}}_{j|j-1}^f \mathbf{1}^\top + \delta\mathbf{X}_{j|j-1}^f \tilde{\mathbf{W}}_j + \delta\mathbf{X}_{j|j-1}^f - \delta\mathbf{X}_{j|j-1}^f \\ &= \mathbf{X}_{j|j-1}^f + \delta\mathbf{X}_{j|j-1}^f (\tilde{\mathbf{W}}_j - \mathbf{I}) \\ &= \mathbf{X}_{j|j-1}^f + \delta\mathbf{X}_{j|j-1}^f \Omega_j. \end{aligned} \quad (27)$$

Considering the  $i$ -th column of  $\mathbf{X}_j^a$ , we obtain Equation (26).  $\square$

Then, based on Lemma 2.1, we provide an approximate equation of the updated forecast ensemble  $\mathbf{X}_{k|j}^f$  derived from the baseline forecast  $\mathbf{X}_{k|0}^f$ .

**Lemma 2.2.** *The forecast ensemble  $\mathbf{X}_{k|j}^f$  for forecast lead time  $k$  updated at forecast reference time  $j$  is represented as follows by the baseline forecast  $\mathbf{X}_{k|0}^f$ , the forecast ensemble perturbations  $\{\delta\mathbf{X}_{k|0}^f, \dots, \delta\mathbf{X}_{k|j-1}^f\}$ , and the matrices  $\{\Omega_1, \dots, \Omega_j\}$ :*

$$\mathbf{X}_{k|j}^f \approx \mathbf{X}_{k|0}^f + \sum_{h=1}^j \delta\mathbf{X}_{k|h-1}^f \Omega_h. \quad (28)$$

*Proof.* From Lemma 2.1, the following equation holds:

$$\begin{aligned}
\mathbf{x}_{k|1}^{f(i)} &= M_{k|1} \left( \mathbf{x}_1^{a(i)} \right) \\
&= M_{k|1} \left( \mathbf{x}_{1|0}^{f(i)} + \sum_{l=1}^m \delta \mathbf{x}_{1|0}^{f(l)} \omega_{1,li} \right) \\
&\approx M_{k|1} \left( \mathbf{x}_{1|0}^{f(i)} \right) + \sum_{l=1}^m \mathbf{M}_{k|1} \delta \mathbf{x}_{1|0}^{f(l)} \omega_{1,li} \\
&= \mathbf{x}_{k|0}^{f(i)} + \sum_{l=1}^m \delta \mathbf{x}_{k|0}^{f(l)} \omega_{1,li}, \tag{29}
\end{aligned}$$

$$\iff \mathbf{X}_{k|1}^f \approx \mathbf{X}_{k|0}^f + \delta \mathbf{X}_{k|0}^f \boldsymbol{\Omega}_1. \tag{30}$$

Therefore, Equation (28) holds for  $j = 1$ . We assume that Equation (28) holds for  $j = t$ . Then, considering the case  $j = t + 1$ , the following equation holds:

$$\begin{aligned}
\mathbf{x}_{k|t+1}^{f(i)} &= M_{k|t+1} \left( \mathbf{x}_{t+1}^{a(i)} \right) \\
&= M_{k|t+1} \left( \mathbf{x}_{t+1|t}^{f(i)} + \sum_{l=1}^m \delta \mathbf{x}_{t+1|t}^{f(l)} \omega_{t+1,li} \right) \\
&\approx M_{k|t+1} \left( \mathbf{x}_{t+1|t}^{f(i)} \right) + \sum_{l=1}^m \mathbf{M}_{k|t+1} \delta \mathbf{x}_{t+1|t}^{f(l)} \omega_{t+1,li} \\
&= \mathbf{x}_{k|t}^{f(i)} + \sum_{l=1}^m \delta \mathbf{x}_{k|t}^{f(l)} \omega_{t+1,li} \\
&\approx \mathbf{x}_{k|0}^{f(i)} + \sum_{h=1}^t \sum_{l=1}^m \delta \mathbf{x}_{k|h-1}^{f(l)} \omega_{h,li} + \sum_{l=1}^m \delta \mathbf{x}_{k|t}^{f(l)} \omega_{t+1,li} \\
&= \mathbf{x}_{k|0}^{f(i)} + \sum_{h=1}^{t+1} \sum_{l=1}^m \delta \mathbf{x}_{k|h-1}^{f(l)} \omega_{h,li}, \tag{31}
\end{aligned}$$

$$\iff \mathbf{X}_{k|t+1}^f \approx \mathbf{X}_{k|0}^f + \sum_{h=1}^{t+1} \delta \mathbf{X}_{k|h-1}^f \boldsymbol{\Omega}_h. \tag{32}$$

Therefore, because it also holds for  $j = t + 1$ , Equation (28) holds for all  $j$ .  $\square$

Subsequently, to represent the updated forecast ensemble  $\mathbf{X}_{k|j}^f$  by the product of ensemble transform matrices, we consider the following lemma.

**Lemma 2.3.** *For the baseline forecast  $\mathbf{X}_{k|0}^f$ , the forecast perturbations  $\{\delta \mathbf{X}_{k|0}^f, \dots, \delta \mathbf{X}_{k|j-1}^f\}$ , the matrices  $\{\boldsymbol{\Omega}_1, \dots, \boldsymbol{\Omega}_j\}$ , and the ensemble transform matrices  $\{\mathbf{W}_1, \dots, \mathbf{W}_j\}$ , the following equation holds:*

$$\mathbf{X}_{k|0}^f + \sum_{h=1}^j \delta \mathbf{X}_{k|h-1}^f \boldsymbol{\Omega}_h \approx \mathbf{X}_{k|0}^f \mathbf{W}_1 \cdots \mathbf{W}_j. \tag{33}$$

*Proof.* Noting that  $\mathbf{1}^\top \mathbf{W}_1 = \mathbf{1}^\top$ , the following equation is derived:

$$\begin{aligned}
\mathbf{X}_{k|0}^f + \delta \mathbf{X}_{k|0}^f \boldsymbol{\Omega}_1 &= \mathbf{X}_{k|0}^f + \delta \mathbf{X}_{k|0}^f (\mathbf{W}_1 - \mathbf{I}) \\
&= \mathbf{X}_{k|0}^f \mathbf{1}^\top \mathbf{W}_1 + \delta \mathbf{X}_{k|0}^f \mathbf{W}_1 \\
&= \mathbf{X}_{k|0}^f \mathbf{W}_1. \tag{34}
\end{aligned}$$

Therefore, Equation (33) holds for  $j = 1$ . We assume that Equation (33) holds for  $j = t$ . Then, considering the case  $j = t + 1$ , the following equation holds from Lemma 2.2:

$$\begin{aligned}
\mathbf{X}_{k|0}^f + \sum_{h=1}^{t+1} \delta \mathbf{X}_{k|h-1}^f \boldsymbol{\Omega}_h &= \mathbf{X}_{k|0}^f + \sum_{h=1}^t \delta \mathbf{X}_{k|h-1}^f \boldsymbol{\Omega}_h + \delta \mathbf{X}_{k|t}^f \boldsymbol{\Omega}_{t+1} \\
&\approx \mathbf{X}_{k|t}^f + \delta \mathbf{X}_{k|t}^f (\tilde{\mathbf{W}}_{t+1} - \mathbf{I}) \\
&= \bar{\mathbf{x}}_{k|t}^f \mathbf{1}^\top \tilde{\mathbf{W}}_{t+1} + \delta \mathbf{X}_{k|t}^f \tilde{\mathbf{W}}_{t+1} \\
&= \mathbf{X}_{k|t}^f \tilde{\mathbf{W}}_{t+1} \\
&\approx \left[ \mathbf{X}_{k|0}^f + \sum_{h=1}^t \delta \mathbf{X}_{k|h-1}^f \boldsymbol{\Omega}_h \right] \tilde{\mathbf{W}}_{t+1} \\
&\approx \mathbf{X}_{k|0}^f \tilde{\mathbf{W}}_1 \cdots \tilde{\mathbf{W}}_{t+1}.
\end{aligned} \tag{35}$$

Therefore, because it also holds for  $j = t + 1$ , Equation (33) holds for all  $j$ .  $\square$

These lemmas lead to the following theorem.

**Theorem 2.4.** *In a nonlinear model, the forecast ensemble  $\mathbf{X}_{k|j}^f$  for forecast lead time  $k$  at forecast reference time  $j$  is expressed as follows using the baseline forecast  $\mathbf{X}_{k|0}^f$  and the ensemble transform matrices  $\{\tilde{\mathbf{W}}_1, \dots, \tilde{\mathbf{W}}_j\}$ :*

$$\mathbf{X}_{k|j}^f \approx \mathbf{X}_{k|0}^f \tilde{\mathbf{W}}_1 \cdots \tilde{\mathbf{W}}_j = \mathbf{X}_{k|0}^f \tilde{\mathbf{W}}_j^{\text{prod}}. \tag{36}$$

*Proof.* This follows immediately from Lemmas 2.2 and 2.3.  $\square$

Introducing localization into URDA implemented by LETKF, Equation (36) is expressed as follows:

$$\mathbf{x}_{k|j,g}^f \approx \mathbf{x}_{k|0,g}^f \tilde{\mathbf{W}}_1^{\text{loc}} \cdots \tilde{\mathbf{W}}_j^{\text{loc}} = \mathbf{x}_{k|0,g}^f \tilde{\mathbf{W}}_j^{\text{prod,loc}}. \tag{37}$$

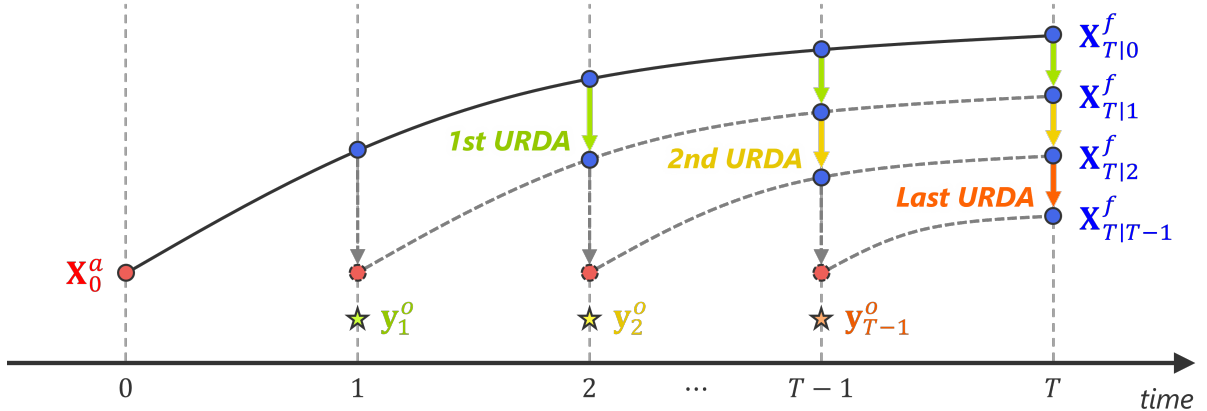


Figure 1: The concept of URDA. A situation is assumed in which the baseline forecast already exists from time 0 to time  $T$ , and additional observations become available at each subsequent time step. URDA sequentially updates the preemptive forecasts using the existing forecast ensembles and the additional observations.

## 2.4 Technical treatments for URDA

In nonlinear models, the preemptive forecasts obtained by URDA are approximate rather than ideal, as in Equation (36). As a result, the following issues arise when URDA is applied to nonlinear models (cf. Section 4.1).

1. The accuracy deteriorates and the spread collapses as the preemptive forecast is repeatedly updated.
2. The deterioration of accuracy and the collapse of spread are caused by extending the forecast lead time. In particular, the accuracy may even deteriorate compared to the baseline forecast.

To mitigate these issues, this study proposes RTBP and RTBF as technical treatments for URDA.

#### 2.4.1 RTBP

RTBP calculates the weighted average of the ensemble transform matrix  $\mathbf{W}_j^{prod} := \mathbf{W}_1 \cdots \mathbf{W}_j$  and the identity matrix  $\mathbf{I}$  as follows:

$$\mathbf{W}_j^{prod,RTBP} := (1 - \alpha^{RTBP}) \mathbf{W}_j^{prod} + \alpha^{RTBP} \mathbf{I}, \quad (38)$$

where  $\alpha$  is a real number in the range  $[0, 1]$  and its superscript denotes that it is a tuning parameter of the inflation technique. Note that  $\mathbf{W}_j^{prod}$  can be decomposed into  $\mathbf{w}_j^{prod}$  and  $\mathbf{W}_j^{prod}$  as follows:

$$\mathbf{W}_j^{prod} = \frac{1}{\sqrt{m-1}} \mathbf{w}_j^{prod} \mathbf{1}^\top + \mathbf{W}_j^{prod}, \quad \mathbf{w}_j^{prod} := \sum_{t=1}^j \mathbf{W}_{t-1}^{prod} \mathbf{w}_t, \quad \mathbf{W}_0^{prod} := \mathbf{I}. \quad (39)$$

Also,  $\mathbf{w}_j^{prod}$  and  $\mathbf{W}_j^{prod}$  can be calculated using the ensemble transform matrix  $\mathbf{\widetilde{W}}_j^{prod}$  as follows:

$$\mathbf{w}_j^{prod} = \frac{\sqrt{m-1}}{m} (\mathbf{\widetilde{W}}_j^{prod} - \mathbf{I}) \mathbf{1}, \quad (40)$$

$$\mathbf{W}_j^{prod} = \mathbf{\widetilde{W}}_j^{prod} - \frac{1}{m} (\mathbf{\widetilde{W}}_j^{prod} - \mathbf{I}) \mathbf{J}, \quad \mathbf{J} := \mathbf{1} \mathbf{1}^\top. \quad (41)$$

For the derivation of Equations (39) – (41), refer to Appendix A. The RTBP formula (38) is similar to the following RTPP formula, which is expressed as:

$$\delta \mathbf{X}_j^{a,RTPP} = (1 - \alpha^{RTPP}) \delta \mathbf{X}_j^a + \alpha^{RTPP} \cdot \delta \mathbf{X}_j^f \iff \mathbf{W}_j^{RTPP} = (1 - \alpha^{RTPP}) \mathbf{W}_j + \alpha^{RTPP} \mathbf{I}, \quad (42)$$

but note that RTBP applies  $\mathbf{W}_j^{prod}$ , not  $\mathbf{W}_j$ . Then, in URDA, RTBP is expected to function more effectively than conventional inflation techniques such as multiplicative inflation, RTPP, and RTPS, as discussed in Section 5.

#### 2.4.2 RTBF

RTBF calculates the weighted average of the ensemble transform matrix  $\mathbf{\widetilde{W}}_j^{prod}$  and the identity matrix  $\mathbf{I}$  as follows:

$$\mathbf{\widetilde{W}}_j^{prod,RTBF} := (1 - \alpha^{RTBF}) \mathbf{\widetilde{W}}_j^{prod} + \alpha^{RTBF} \mathbf{I}. \quad (43)$$

From Equation (36), we find that the preemptive forecast is relaxed toward the baseline forecast as  $\alpha^{RTBF}$  approaches 1 in RTBF.

#### 2.4.3 URDA with RTBP and RTBF

The algorithm of the proposed URDA is presented in Algorithm 1. We apply RTBP to the ensemble transform matrix  $\mathbf{W}_{j-1}^{prod,loc}$  at each forecast reference time  $j$ . RTBP is expected to mitigate the deterioration in accuracy and the collapse of the spread caused by repeated updates of the preemptive forecast. Note that, at time  $j$ , RTBP is applied to the ensemble transform matrix  $\mathbf{W}_{j-1}^{prod,loc}$ , not to  $\mathbf{W}_j^{prod,loc}$ . This is because preliminary experiments confirmed that applying RTBP to  $\mathbf{W}_{j-1}^{prod,loc}$  rather than  $\mathbf{W}_j^{prod,loc}$  resulted in better accuracy and spread in the initial forecast  $\mathbf{X}_{j+1|j}^f$ . We speculate that the role of RTBP is not only to inflate the spread but also to gradually forget information from the old ensemble transform matrix  $\mathbf{W}_{j-1}^{prod,loc}$ , thereby enhancing the components of the current

ensemble transform matrix  $\mathbf{W}_j^{loc}$ , which is considered important. However, in this case, even if  $\alpha^{RTBP}$  is set to 1, the preemptive forecast's perturbation is no longer consistent with the baseline forecast's perturbation. Therefore, while it may not strictly qualify as RTBP, we continue to use the term RTBP for convenience. In addition, while it is conceivable to apply RTBF instead of RTBP for each forecast reference time  $j$ , preliminary experiments showed that RTBP yielded better results than RTBF for the initial forecast  $\mathbf{X}_{j+1|j}^f$ . Therefore, RTBP is employed for this purpose in this study.

In conventional URDA, the same ensemble transform matrix  $\tilde{\mathbf{W}}_j^{prod,loc}$  is applied for all forecast lead times  $j+1 \leq k \leq T$  at forecast reference time  $j$ . However, in this algorithm, RTBF is applied for each forecast lead time  $k$ . As a result, the ensemble transform matrix applied to the baseline forecast gradually converges to the identity matrix. Therefore, although it may not lead to improvements, it can at least be expected to prevent a sharp deterioration in accuracy and collapse of the spread caused by extending the forecast lead time.

---

**Algorithm 1** URDA with RTBP and RTBF

---

Step 1. Compute the ensemble transform matrix  $\tilde{\mathbf{W}}_{j-1}^{prod,loc}$  for forecast reference time  $j-1$  by RTBP as follows:

$$\begin{aligned}\mathbf{w}_{j-1}^{prod,loc} &\leftarrow \frac{\sqrt{m-1}}{m} \left( \tilde{\mathbf{W}}_{j-1}^{prod,loc} - \mathbf{I} \right) \mathbf{1}, \\ \mathbf{W}_{j-1}^{prod,loc} &\leftarrow \tilde{\mathbf{W}}_{j-1}^{prod,loc} - \frac{1}{m} \left( \tilde{\mathbf{W}}_{j-1}^{prod,loc} - \mathbf{I} \right) \mathbf{J}, \\ \mathbf{W}_{j-1}^{prod,loc,RTBP} &\leftarrow (1 - \alpha^{RTBP}) \mathbf{W}_{j-1}^{prod,loc} + \alpha^{RTBP} \mathbf{I}, \\ \tilde{\mathbf{W}}_{j-1}^{prod,loc} &\leftarrow \frac{1}{\sqrt{m-1}} \mathbf{w}_{j-1}^{prod,loc} \mathbf{1}^\top + \mathbf{W}_{j-1}^{prod,loc,RTBP}.\end{aligned}$$

Step 2. Compute the ensemble transform matrix  $\tilde{\mathbf{W}}_j^{prod,loc}$  for forecast reference time  $j$ :

$$\tilde{\mathbf{W}}_j^{prod,loc} \leftarrow \tilde{\mathbf{W}}_{j-1}^{prod,loc} \tilde{\mathbf{W}}_j^{loc}.$$

Step 3. Compute the ensemble transform matrix  $\tilde{\mathbf{W}}_j^{prod,loc,RTBF}$  by RTBF and the forecast ensemble  $\mathbf{x}_{k|j,g}^f$  at the  $g$ -th grid point in the range of forecast lead time  $j+1 \leq k \leq T$ :

$$\begin{aligned}\tilde{\mathbf{W}}_j^{prod,loc,RTBF} &\leftarrow (1 - \alpha^{RTBF}) \tilde{\mathbf{W}}_j^{prod,loc} + \alpha^{RTBF} \mathbf{I}, \\ \mathbf{x}_{k|j,g}^f &\leftarrow \mathbf{x}_{k|0,g}^f \tilde{\mathbf{W}}_j^{prod,loc,RTBF}, \\ \tilde{\mathbf{W}}_j^{prod,loc} &\leftarrow \tilde{\mathbf{W}}_j^{prod,loc,RTBF}, \\ k &\leftarrow k + 1.\end{aligned}$$

Step 4. Proceed to the next forecast reference time  $j+1$ :

$$j \leftarrow j + 1.$$


---

### 3 EXPERIMENT

#### 3.1 The Lorenz 96 model

In this study, numerical experiments with URDA are conducted using the 40-variable Lorenz 96 model, a chaotic dynamical system. The Lorenz 96 model can be regarded as mimicking certain physical quantities distributed uniformly on the same latitude circle (Lorenz and Emanuel, 1998). The equations of the Lorenz 96 model are represented as differential equations composed of advection terms, dissipation terms, and forcing terms that are intrinsic to meteorological phenomena, as follows:

$$\frac{dx_g}{dt} = (x_{g+1} - x_{g-2}) x_{g-1} - x_g + F, \quad g = 1, \dots, n, \quad (44)$$

where the dimension of the model space is  $n = 40$  and the forcing term is set to  $F = 8.0$  to induce chaotic behavior in the system. The system is numerically integrated using a fourth-order Runge–Kutta scheme. One time step in the integration is defined as a dimensionless time unit,  $dt = 0.01$ . In the Lorenz 96 model with  $F = 8.0$ , one unit of time corresponds to 5 days (i.e.,  $dt = 0.01$  unit of time corresponds to 1.2 hours) based on the discussion of error doubling time by Lorenz and Emanuel (1998).

### 3.2 Conventional technical treatments

As conventional inflation techniques for URDA, this study employs multiplicative inflation, RTPP, and RTPS. Multiplicative inflation is applied as follows:

$$\delta \mathbf{X}_j^{f, \text{multi}} := \delta \cdot \delta \mathbf{X}_j^f, \quad (45)$$

where  $\delta$  is a real number greater than or equal to 1, serving as a tuning parameter for multiplicative inflation. Additionally, RTPP and RTPS are applied as follows:

$$\delta \mathbf{X}_j^{a, \text{RTPP}} := (1 - \alpha^{\text{RTPP}}) \delta \mathbf{X}_j^a + \alpha^{\text{RTPP}} \delta \mathbf{X}_j^f, \quad (46)$$

$$\delta \mathbf{x}_{j,g}^{a, \text{RTPS}} := \left( \alpha^{\text{RTPS}} \frac{\sigma_{j,g}^f - \sigma_{j,g}^a}{\sigma_{j,g}^a} + 1 \right) \delta \mathbf{x}_{j,g}^a, \quad (47)$$

where  $\sigma_{j,g}^f$  and  $\sigma_{j,g}^a$  denote the prior and posterior ensemble standard deviations at the  $g$ -th grid point, respectively.

In this study, we apply localization to the observation error covariance matrix  $\mathbf{R}$ . The following Gaussian function is employed as the localization function:

$$L(d) = \begin{cases} \exp\left(-\frac{d^2}{2\sigma^2}\right) & \text{if } d < 2\sigma\sqrt{\frac{10}{3}} \\ 0 & \text{otherwise} \end{cases}, \quad (48)$$

where  $d$  denotes the distance between an analysis grid point and an observation.

### 3.3 Experimental design of URDA

The experimental design of URDA is outlined as follows.

1. An observing system simulation experiment (OSSE) is performed to save the true states and analysis ensembles.
2. URDA experiments are conducted using observations and baseline forecasts generated from the saved true states and analysis ensembles, respectively.

As preparation for the URDA experiments, the OSSE procedure is described. First, a one-year spin-up is performed, followed by a two-year plus 30-day integration of the Lorenz 96 model, which is saved as the true state. Then, observations for the OSSE are generated by adding Gaussian noise  $\mathcal{N}(0, 1)$  to the true state. Here, the dimension of the observation space is  $p = n$ , the observation interval is  $\Delta t = 0.05$ , and the observation operator is the identity matrix. Subsequently, the assimilation and forecast cycles are performed. LETKF is employed as the data assimilation method, with an ensemble size of 10 members. The multiplicative inflation factor  $\delta$  and the localization scale  $\sigma$  were tuned, with values of  $\delta = 1.03$  and  $\sigma = 5.5$  selected, respectively. The forecast ensemble at the initial time was generated by adding Gaussian noise  $\mathcal{N}(0, 1)$  to the true state, similar to the observations. To avoid using poor-quality analysis ensembles, the data from the first 30 days is removed. Accordingly, the true state from the first 30 days is also removed. Furthermore, to provide independent initial values for the URDA experiments, 293 steps of true states and analysis ensembles extracted every 60 hours from the remaining two years are saved.

Then, the procedure for the URDA experiments is explained. From the 293 steps of the true states and analysis ensembles saved in the OSSE, the  $t$ -th step is extracted and used as the true state  $\mathbf{x}_0^{tru}$  and the analysis ensemble  $\mathbf{X}_0^a$  at the initial time in the time interval  $[0, T]$ . The end of the time interval is set to  $T = 32$  days, a long period. It is intended to evaluate the behavior of URDA over the period until forecast accuracy sufficiently converges. Subsequently, the baseline forecast  $\mathbf{X}_{k|0}^f$  ( $0 < k \leq T$ ) is computed by integrating the Lorenz 96 model from the analysis ensemble  $\mathbf{X}_0^a$ . In the same manner, the true state  $\mathbf{x}_j^{tru}$  ( $0 < j \leq T$ ) is computed. Then, the observation  $\mathbf{y}_j^o$  used in the URDA experiments is generated by adding Gaussian noise  $\mathcal{N}(0, 1)$  to the true state  $\mathbf{x}_j^{tru}$ . The settings

regarding observation, such as observation interval, observation dimension, and observation operator, are basically consistent with the previous OSSE. Then, URDA is performed using the baseline forecast  $\mathbf{X}_{k|0}^f$  and the observation  $\mathbf{y}_j^o$ . This process is applied to all stored data for  $t = 1, \dots, 293$  steps, and statistical evaluations are eventually conducted for performance metrics such as the root mean square error (RMSE) and the spread.

## 4 RESULTS

### 4.1 The conventional URDA

Here, we present the RMSE, spread, and the ensemble transform matrix  $\tilde{\mathbf{W}}_j^{prod,loc}$  to highlight the difficulties of the conventional URDA (i.e., URDA with conventional inflation techniques) in nonlinear models. As a representative example, the results for a multiplicative inflation factor  $\delta = 1.05$  and a localization scale  $\sigma = 1.0$  are shown.

Figure 2 shows the RMSE and spread of the preemptive forecast  $\mathbf{X}_{k|j}^f$  with the conventional URDA for each forecast lead time  $k$  at each forecast reference time  $j$ . For the RMSE, it is found that accuracy tends to deteriorate each time the preemptive forecast is updated by the conventional URDA. Specifically, focusing on the initial forecasts for each forecast reference time (dash-dotted line)  $\mathbf{X}_{j+1|j}^f$ , the accuracy improves compared to the baseline forecast (dashed line)  $\mathbf{X}_{k|0}^f$  during the early part of the forecast reference time. However, as the forecast reference time approaches its end, the accuracy of the initial forecasts  $\mathbf{X}_{j+1|j}^f$  asymptotically approaches that of the baseline forecast  $\mathbf{X}_{k|0}^f$ , thereby significantly diminishing the improvement in accuracy. Furthermore, extending the forecast lead time causes accuracy to deteriorate sharply at any forecast reference time, leading to a significant deterioration compared to the baseline forecast. In addition, it is found that the spread tends to collapse each time the preemptive forecast is updated by the conventional URDA. In particular, during the latter part of the forecast reference time, the spread hardly increases even though the forecast lead time is extended.

The preemptive forecast of URDA with localization is fundamentally prescribed by the ensemble transform matrix  $\tilde{\mathbf{W}}_j^{prod,loc}$ , as shown in Equation (37). Thus, Figure 3 shows the ensemble transform matrix  $\tilde{\mathbf{W}}_j^{prod,loc}$  of the conventional URDA for each forecast reference time at grid point  $g = 0$  as an example. In the early part of the forecast reference time, the diagonal elements are dominant, and the off-diagonal elements also exhibit moderate fluctuations. However, each time the preemptive forecast is updated (i.e., the ensemble transform matrix  $\tilde{\mathbf{W}}_j^{loc}$  is multiplied), the diagonal elements gradually decrease, and the elements in each row become more homogeneous. This homogenization of the elements in each row may cause the deterioration in the RMSE and the collapse of the spread, particularly for the initial forecast  $\mathbf{X}_{j+1|j}^f$ . This point is discussed in detail in Section 5.

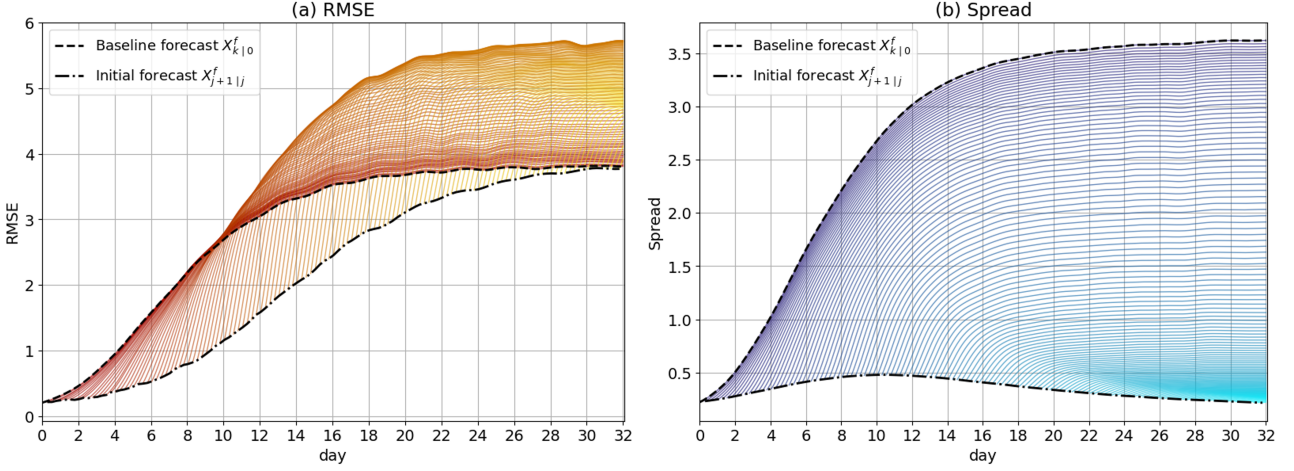


Figure 2: The RMSE and the spread of the conventional URDA (multiplicative inflation factor  $\delta = 1.05$  and localization scale  $\sigma = 1.0$ ). In both figures, each solid line represents the preemptive forecast  $\mathbf{X}_{k|j}^f$  for each forecast lead time  $k$  at each forecast reference time  $j$ . The dashed line represents the baseline forecast  $\mathbf{X}_{k|0}^f$ , and the dash-dotted line represents the initial forecast  $\mathbf{X}_{j+1|j}^f$  for each forecast reference time. (a) Dark and light red solid lines show the RMSE for the early and latter parts of the forecast reference time. (b) Dark and light blue solid lines show the spread for the early and latter parts of the forecast reference time.

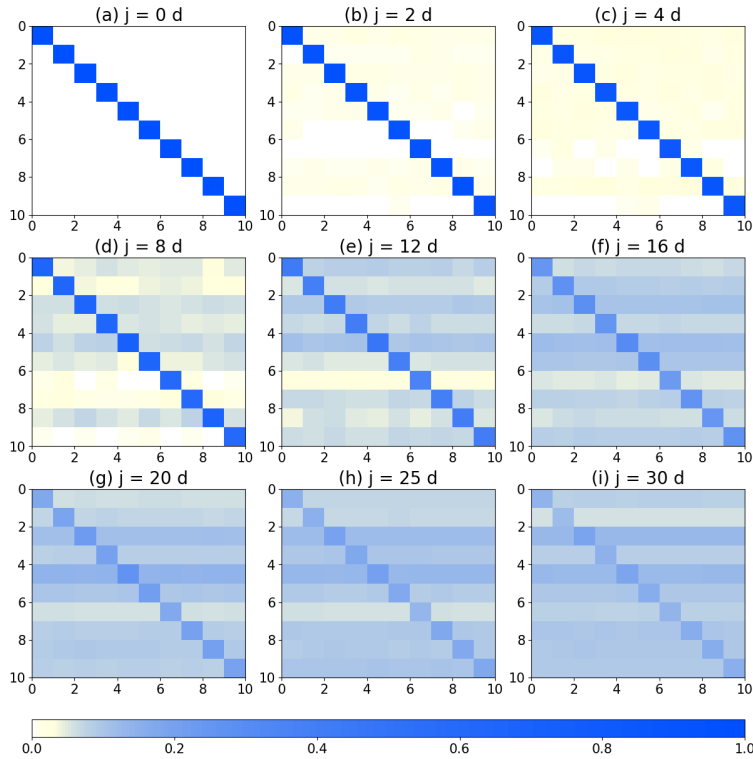


Figure 3: The ensemble transform matrix  $\tilde{\mathbf{W}}_j^{prod,loc}$  of the conventional URDA (multiplicative inflation factor  $\delta = 1.05$  and localization scale  $\sigma = 1.0$ ) for each forecast reference time from (a)  $j = 0$  days to (i)  $j = 30$  days at grid point  $g = 0$ .

## 4.2 Investigation of inflation and localization

We investigate the properties of URDA with respect to inflation and localization. Specifically, we conduct sensitivity experiments on the inflation factor and localization scale, evaluating the RMSE of the initial forecast  $\mathbf{X}_{j+1|j}^f$  for each forecast reference time. As inflation techniques, multiplicative

inflation, RTPP, and RTPS are employed.

Figure 4 shows the RMSE of the initial forecast  $\mathbf{X}_{j+1|j}^f$  for each forecast reference time with respect to the multiplicative inflation factor  $\delta$  and localization scale  $\sigma$ . This result indicates that there is no significant sensitivity to the multiplicative inflation factor  $\delta$ . Therefore, although the spread collapses with the inflation factor  $\delta = 1.05$  in Figure 2, increasing the inflation factor does not provide an effective solution. It is found, rather, that the inflation factor  $\delta = 1.0$  yields the smallest overall RMSE. In addition, regarding the localization scale  $\sigma$ , it is found that a relatively large localization scale  $\sigma$  yields a lower RMSE in the early part of the forecast reference time, whereas a smaller localization scale  $\sigma$  becomes more effective as the forecast reference time approaches its latter part.

Figure 5 indicates the RMSE of the initial forecast  $\mathbf{X}_{j+1|j}^f$  for each forecast reference time regarding the inflation factor  $\alpha^{RTPP}$  and localization scale  $\sigma$ . Compared to multiplicative inflation, RTPP offers a lower minimum RMSE for each forecast reference time, indicating that RTPP is more effective for the RMSE of the initial forecast  $\mathbf{X}_{j+1|j}^f$ . It is found that the best inflation factor  $\alpha^{RTPP}$  increases as the forecast reference time progresses. Regarding the localization scale  $\sigma$ , it shows a similar pattern to that in the case of multiplicative inflation.

Figure 6 shows the RMSE of the initial forecast  $\mathbf{X}_{j+1|j}^f$  for each forecast reference time with respect to the inflation factor  $\alpha^{RTPS}$  and localization scale  $\sigma$ . At any forecast reference time, increasing the inflation factor  $\alpha^{RTPS}$  causes a sharp deterioration or numerical instability, clearly demonstrating that RTPS is unsuitable for URDA.

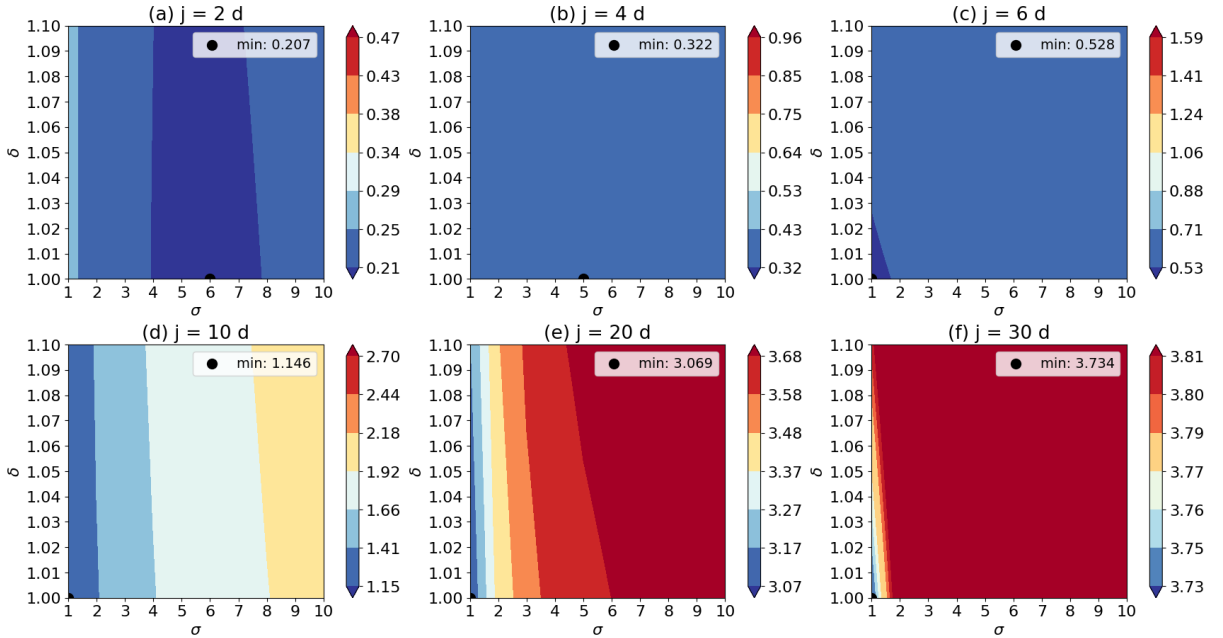


Figure 4: The RMSE of the initial forecast  $\mathbf{X}_{j+1|j}^f$  at each forecast reference time from (a) 2 days to (f) 30 days for the multiplicative inflation factor  $\delta$  and localization scale  $\sigma$ . The black dots indicate the minimum RMSE at each forecast reference time.

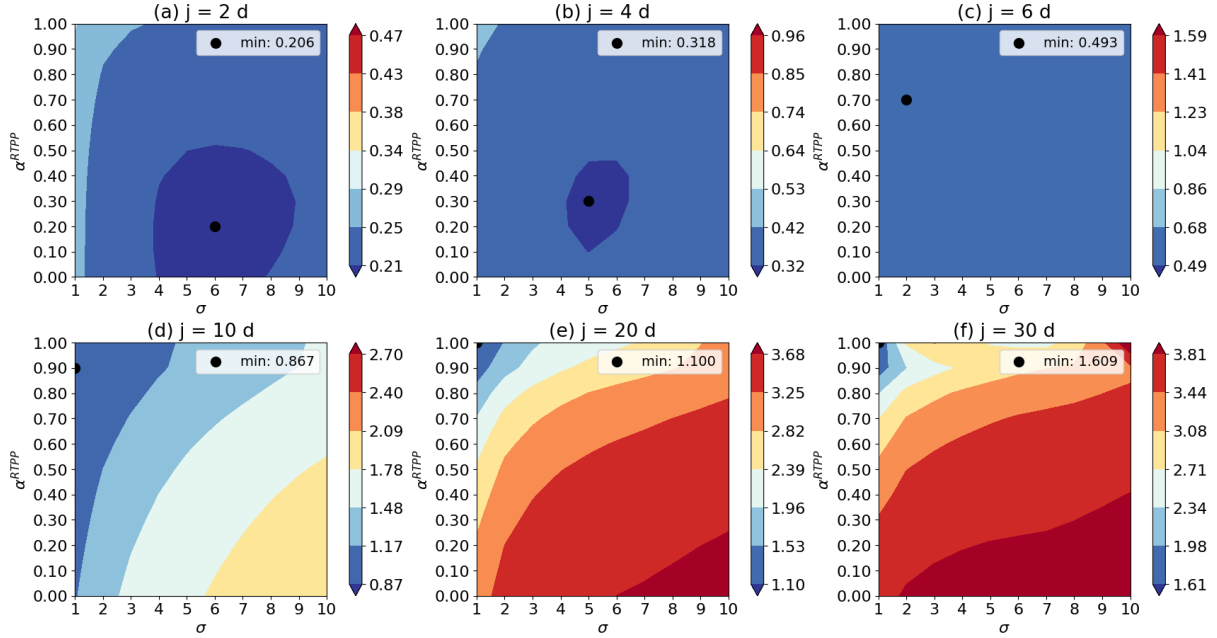


Figure 5: Similar to Figure 4, but for the inflation factor  $\alpha^{RTPP}$ .

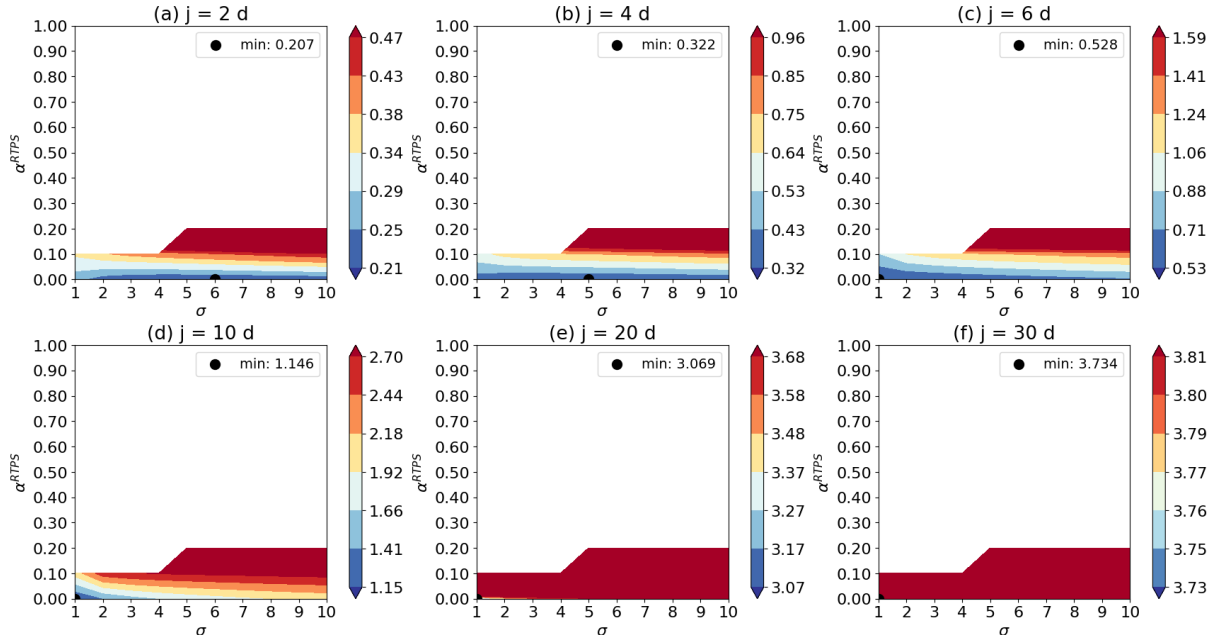


Figure 6: Similar to Figure 4, but for the inflation factor  $\alpha^{RTPS}$ . The white area indicates cases where no result is obtained due to numerical instability.

### 4.3 The proposed URDA

We demonstrate that the proposed URDA (i.e., URDA with RTBP and RTBF) mitigates the difficulties inherent in the conventional URDA. First, as a representative example, we show the RMSE, spread, and ensemble transform matrix  $\tilde{\mathbf{W}}_j^{prod,loc}$  of URDA with inflation factor  $\alpha^{RTBP} = 0.3$ , inflation factor  $\alpha^{RTBF} = 0.1$ , and localization scale  $\sigma = 1.0$ . Subsequently, the results of sensitivity experiments with respect to the inflation factor  $\alpha^{RTBP}$  and localization scale  $\sigma$  are presented. For simplicity, the inflation factor of RTBF was manually tuned in preliminary experiments and fixed at  $\alpha^{RTBF} = 0.1$  throughout this study.

Figure 7 shows the RMSE and the spread of the preemptive forecast  $\mathbf{X}_{k|j}^f$  based on the proposed URDA for each forecast lead time  $k$  at each forecast reference time  $j$ . For the RMSE, it is found

that the initial forecast (dash-dotted line)  $\mathbf{X}_{j+1|j}^f$  is substantially improved compared to the baseline forecast (dashed line)  $\mathbf{X}_{k|0}^f$  at all forecast reference times. Furthermore, even though the forecast lead time is extended, the RMSE of the preemptive forecast  $\mathbf{X}_{k|j}^f$  converges to that of the baseline forecast  $\mathbf{X}_{k|0}^f$ , preventing its deterioration beyond the baseline forecast  $\mathbf{X}_{k|0}^f$ . Regarding the spread, it is seen that the spread of the initial forecast  $\mathbf{X}_{j+1|j}^f$  inflates even though the preemptive forecast is repeatedly updated. Furthermore, at each forecast reference time, the spread converges to that of the baseline forecast  $\mathbf{X}_{k|0}^f$  as the forecast lead time is extended.

As an example, Figure 8 shows the ensemble transform matrix  $\tilde{\mathbf{W}}_j^{prod,loc}$  of the proposed URDA at grid point  $g = 0$  for each forecast reference time, as well as that for each forecast lead time at the forecast reference time of 16 days. At each forecast reference time, the diagonal elements dominate, and the off-diagonal elements fluctuate moderately due to the application of RTBP. That is, unlike the conventional URDA, the homogenization of the elements in each row is prevented even though the ensemble transform matrix  $\tilde{\mathbf{W}}_j^{loc}$  is repeatedly multiplied. Additionally, for each forecast lead time at the forecast reference time of 16 days, the ensemble transform matrix  $\tilde{\mathbf{W}}_j^{prod,loc}$  converges to the identity matrix due to the application of RTBF.

Figure 9 shows the RMSE of the initial forecast  $\mathbf{X}_{j+1|j}^f$  for each forecast reference time with respect to the inflation factor  $\alpha^{RTBP}$  and localization scale  $\sigma$ . It is found that a smaller inflation factor  $\alpha^{RTBP}$  is preferable in the early part of the forecast reference time, while a larger one becomes more effective as the forecast reference time approaches its latter part. It can be stated that RTBP shows robustness, because the range of the best inflation factor over the forecast reference time is narrower (0 to 0.3) than that for RTPP (0.2 to 1.0). For the localization scale  $\sigma$ , it exhibits behavior similar to that in the case of the conventional inflation techniques.

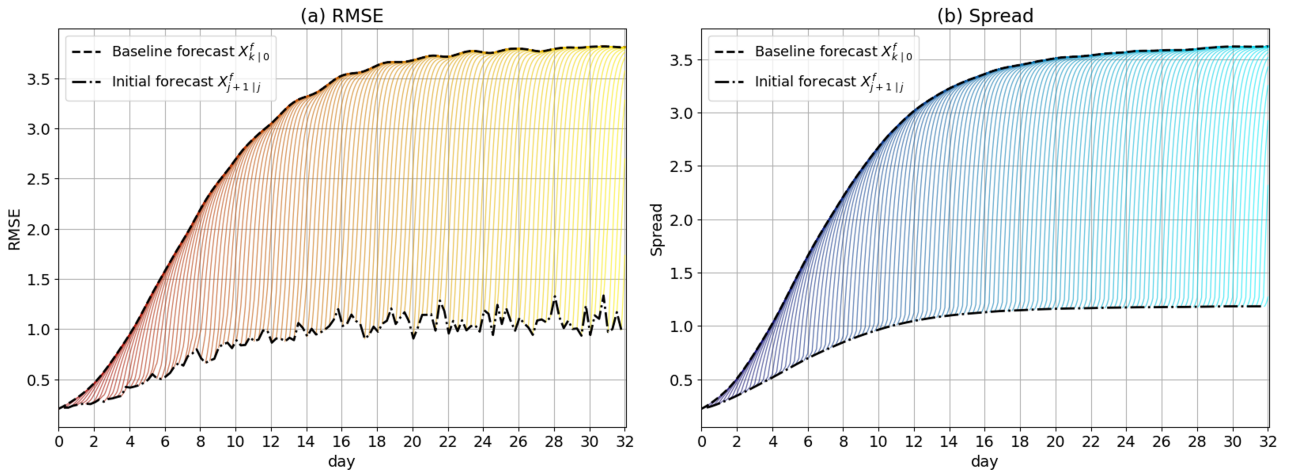


Figure 7: Similar to Figure 2, but for the proposed URDA (inflation factor  $\alpha^{RTBP} = 0.3$ , inflation factor  $\alpha^{RTBF} = 0.1$ , and localization scale  $\sigma = 1.0$ ).

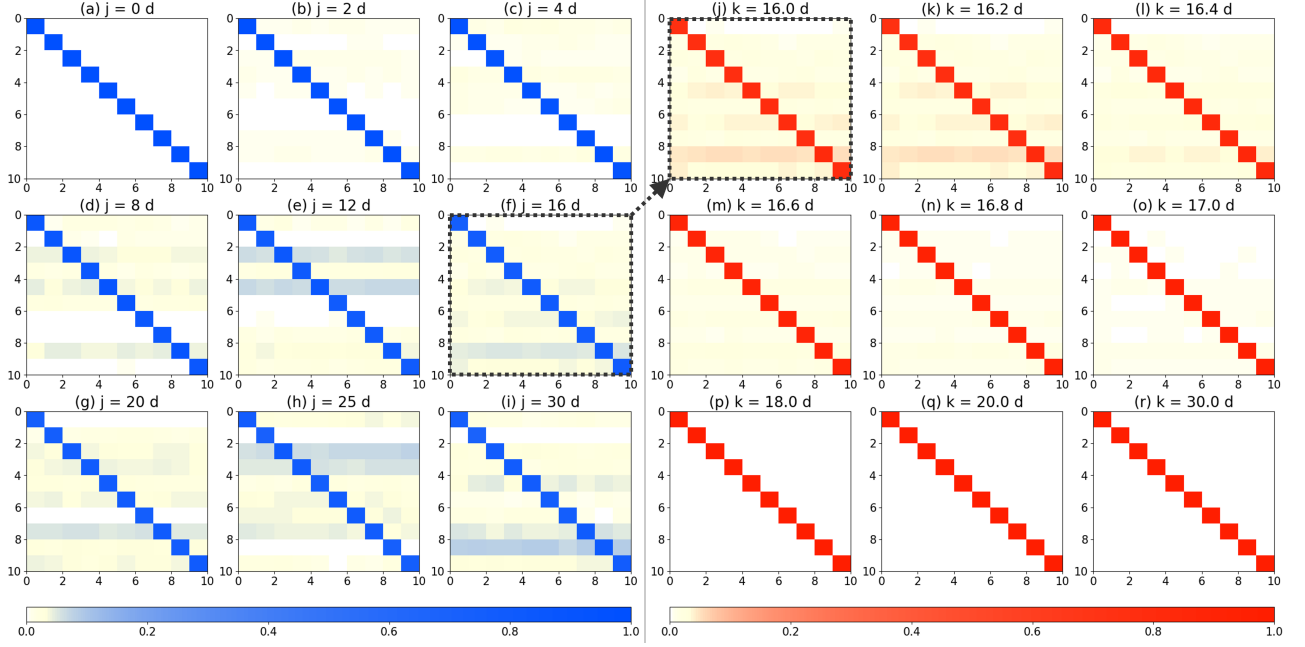


Figure 8: Ensemble transform matrix  $\tilde{\mathbf{W}}_j^{prod,loc}$  of the proposed URDA (inflation factor  $\alpha^{RTBP} = 0.3$ , inflation factor  $\alpha^{RTBF} = 0.1$ , and localization scale  $\sigma = 1.0$ ) at grid point  $g = 0$ . (a-i) The ensemble transform matrix  $\tilde{\mathbf{W}}_j^{prod,loc}$  for each forecast reference time. (j-r) The ensemble transform matrix  $\tilde{\mathbf{W}}_j^{prod,loc}$  for each forecast lead time at the forecast reference time of 16 days. That is, (f) is identical to (j).

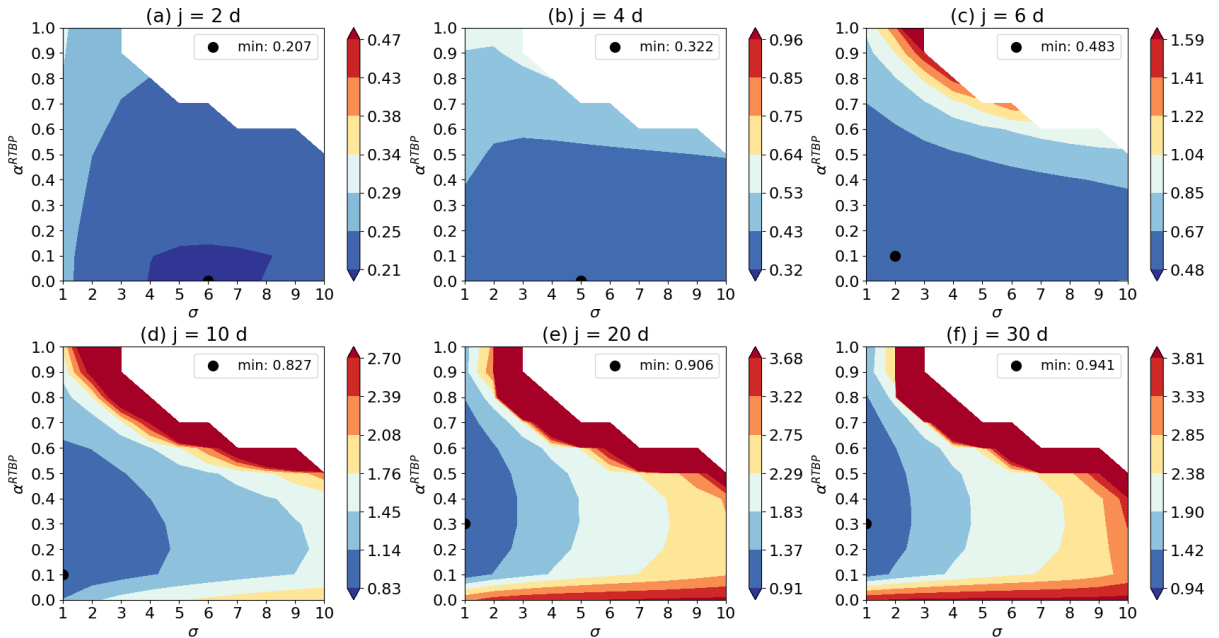


Figure 9: Similar to Figure 4, but for the inflation factor  $\alpha^{RTBP}$ . The white area shows cases where no result is obtained due to numerical instability.

#### 4.4 Comparison of the conventional and proposed URDAs

Finally, we compare the URDA incorporating conventional inflation techniques, such as multiplicative inflation, RTPP, and RTPS, with the URDA incorporating RTBP and RTBF. Here, we evaluate the RMSE and spread from the perspective of the initial forecast  $\mathbf{X}_{j+1|j}^f$  and the last forecast  $\mathbf{X}_{T|j}^f$  at each forecast reference time. The parameters selected here represent the values that yield the best accuracy

of the initial forecast  $\mathbf{X}_{j+1|j}^f$  at a forecast reference time of 30 days for each inflation technique. As a result, the settings for multiplicative inflation and RTPS are equivalent to those without inflation applied; thus, we refer to these settings as no inflation here.

Figure 10 shows a comparison of the RMSE and spread of the initial forecast  $\mathbf{X}_{j+1|j}^f$  and the last forecast  $\mathbf{X}_{T|j}^f$  at each forecast reference time for each inflation technique. The RMSE for no inflation deteriorates significantly, while the spread collapses, indicating a substantial discrepancy between them for both the initial forecast  $\mathbf{X}_{j+1|j}^f$  and the last forecast  $\mathbf{X}_{T|j}^f$ . In RTPP, the RMSE of the initial forecast  $\mathbf{X}_{j+1|j}^f$  is generally lower than that of no inflation. However, the spread inflates to the equivalent of the baseline forecast  $\mathbf{X}_{k|0}^f$  since the inflation factor of RTPP is  $\alpha^{RTPP} = 1.0$ , resulting in a significant discrepancy between them, like the no inflation case. On the other hand, the last forecast  $\mathbf{X}_{T|j}^f$  of RTPP shows that the RMSE deteriorates sharply compared to the no inflation case and the spread is consistent with that of the baseline forecast  $\mathbf{X}_{k|0}^f$ . In both the initial forecast  $\mathbf{X}_{j+1|j}^f$  and the last forecast  $\mathbf{X}_{T|j}^f$  of RTBP and RTBF, the RMSE is generally lower than that of no inflation and RTPP, and the spread appropriately inflates to a degree equivalent to the RMSE. Note that for the last forecast  $\mathbf{X}_{T|j}^f$  in either inflation technique, the reduction of RMSE and spread toward the end of the forecast reference time is due to insufficient evolution of the preemptive forecast as the forecast lead time shortens.

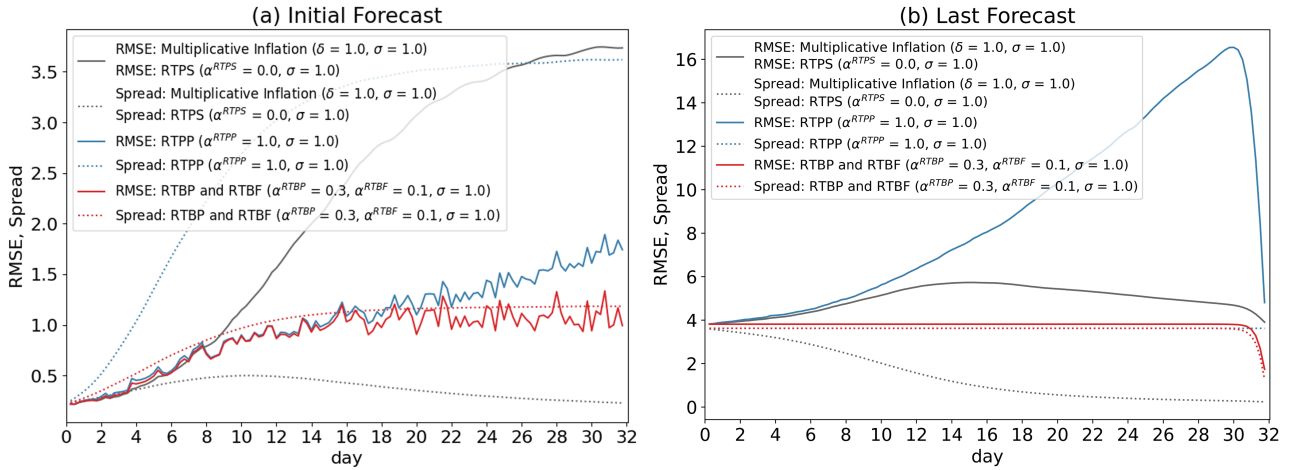


Figure 10: Comparison of RMSE and spread for each inflation technique. The solid lines indicate RMSE, and the dotted lines indicate spread. The black lines represent multiplicative inflation (multiplicative inflation factor  $\delta = 1.0$  and localization scale  $\sigma = 1.0$ ) or RTPS (inflation factor  $\alpha^{RTPS} = 0$  and localization scale  $\sigma = 1.0$ ), i.e., no inflation. The blue lines represent RTPP (inflation factor  $\alpha^{RTPP} = 1.0$  and localization scale  $\sigma = 1.0$ ). The red lines represent RTBP and RTBF (inflation factor  $\alpha^{RTBP} = 0.3$ , inflation factor  $\alpha^{RTBF} = 0.1$ , and localization scale  $\sigma = 1.0$ ). (a) RMSE and spread of the initial forecast  $\mathbf{X}_{j+1|j}^f$  at each forecast reference time. (b) RMSE and spread of the last forecast  $\mathbf{X}_{T|j}^f$  at each forecast reference time.

## 5 DISCUSSION

### 5.1 Difficulties with the conventional URDA

One major difficulty with the conventional URDA in nonlinear models is that repeated updates of the preemptive forecast lead to a deterioration in the RMSE and a collapse of the ensemble spread. As shown in Figure 3, the elements in each row of the ensemble transform matrix  $\widetilde{\mathbf{W}}_j^{prod,loc}$  become more homogeneous each time the ensemble transform matrix  $\widetilde{\mathbf{W}}_j^{loc}$  is multiplied in the conventional URDA. Multiplying the baseline forecast  $\mathbf{X}_{k|0}^f$  by such a matrix from the right, as in Equation (36), tends to yield a preemptive forecast  $\mathbf{X}_{k|j}^f$  each of whose rows becomes more homogeneous. Conse-

quently, the spread collapses, which likely causes the deterioration of the RMSE as shown in Figure 2. Furthermore, the deterioration of the RMSE caused by repeatedly updating the preemptive forecast may also be attributed to the linear approximation of URDA in nonlinear models. Another difficulty of the conventional URDA in nonlinear models is a significant deterioration in the RMSE compared to the baseline forecast  $\mathbf{X}_{k|0}^f$  as the forecast lead time is extended. As shown in Equation (36), the preemptive forecast of URDA is expressed as a linear combination of the baseline forecast  $\mathbf{X}_{k|0}^f$  with an ensemble transform matrix  $\tilde{\mathbf{W}}_j^{prod,loc}$ . Therefore, the preemptive forecast may deviate from the attractor, and this likely causes the sharp deterioration in the RMSE with longer forecast lead time.

As shown in Figure 4, it is found that multiplicative inflation is ineffective in improving URDA performance. Indeed, the smallest RMSE is obtained with the multiplicative inflation factor  $\delta = 1.0$  at each forecast reference time. This is likely because, even when multiplicative inflation is applied at each forecast reference time, the elements in each row rapidly become more homogeneous when the ensemble transform matrix  $\tilde{\mathbf{W}}_j^{loc}$  is multiplied repeatedly. Furthermore, this suggests that bringing the ensemble transform matrix  $\tilde{\mathbf{W}}_j^{loc}$  closer to the identity matrix is effective for preventing the elements of each row from becoming homogeneous, even though the ensemble transform matrix  $\tilde{\mathbf{W}}_j^{loc}$  is multiplied repeatedly. In addition, as shown in Figure 6, it is found that RTPS also performs poorly, similar to multiplicative inflation. This is because, as shown in Appendix A, the ensemble transform matrix  $\tilde{\mathbf{W}}_j^{prod}$  possesses the property  $\mathbf{1}^\top \tilde{\mathbf{W}}_j^{prod} = \mathbf{1}^\top$  regarding the sum of columns, but applying RTPS violates this property. As shown in Figure 5, RTPP performs better than these inflation techniques. However, when compared to RTBP, the accuracy of the initial forecast  $\mathbf{X}_{j+1|j}^f$  with RTPP is lower as shown in Figure 10. As previously noted, it is suggested that bringing the ensemble transform matrix  $\tilde{\mathbf{W}}_j^{loc}$  closer to the identity matrix is effective for preventing the homogenization of the elements in each row, even though the ensemble transform matrix  $\tilde{\mathbf{W}}_j^{loc}$  is multiplied repeatedly. Then, rather than taking the weighted average with the identity matrix for each ensemble transform matrix  $\tilde{\mathbf{W}}_j^{loc}$  before multiplication, it is more effective to compute the ensemble transform matrix  $\tilde{\mathbf{W}}_j^{prod,loc}$  and then take the weighted average with the identity matrix, thereby bringing it closer to the identity matrix more efficiently. This might be why RTBP is superior to RTPP.

## 5.2 Effectiveness and limitations of the proposed URDA

The proposed URDA demonstrates that the difficulties of the conventional URDA in nonlinear models are mitigated. Specifically, as shown in Figure 8a-i, applying RTBP at each forecast reference time prevents the homogenization of the elements in each row of the ensemble transform matrix  $\tilde{\mathbf{W}}_j^{prod,loc}$ , even though the ensemble transform matrix  $\tilde{\mathbf{W}}_j^{loc}$  is repeatedly multiplied. This would mitigate the deterioration of the RMSE and the collapse of the spread caused by repeatedly updating the preemptive forecast. However, as shown in Figure 9, the best parameters differ depending on the forecast reference time. Therefore, if the parameters could be adaptively optimized for each forecast reference time, the accuracy could potentially be further improved. In addition, as shown in Figure 8j-r, applying RTBF at each forecast lead time causes the ensemble transform matrix  $\tilde{\mathbf{W}}_j^{prod,loc}$  to converge to the identity matrix as the forecast lead time is extended. That is, as shown in Equation (36), the preemptive forecast converges to the baseline forecast  $\mathbf{X}_{k|0}^f$  as the forecast lead time is extended. This would prevent the substantial deterioration of the RMSE against the baseline forecast  $\mathbf{X}_{k|0}^f$  caused by extending the forecast lead time. However, although the deterioration is prevented, the error growth of the preemptive forecast is rapid, and thus it quickly converges to the baseline forecast  $\mathbf{X}_{k|0}^f$ . Therefore, a limitation of URDA in this study is that its benefits are confined to short forecast lead times.

Since this study is based on idealized numerical experiments using the 40-variable Lorenz 96 model, there are limitations in evaluating the applicability and effectiveness of the proposed URDA for NWP. For example, in this experiment, the baseline forecast period is set to 32 days, which is an impractically long duration, to ensure a stable evaluation period. However, the homogenization of the elements in each row of the ensemble transform matrix  $\tilde{\mathbf{W}}_j^{prod,loc}$  is probably due to the number of times the

ensemble transform matrix  $\tilde{\mathbf{W}}_j^{loc}$  is multiplied rather than the length of the baseline forecast period. Therefore, it is likely that setting an unrealistically long baseline forecast period does not undermine the effectiveness of the proposed method. Additionally, previous studies employing the predecessor of URDA (Etherton, 2007; Madaus and Hakim, 2015) demonstrated improvements in forecast accuracy even with realistic NWP models. Therefore, while further studies are required to verify the proposed URDA using realistic meteorological models, it would be promising for practical applications in NWP.

## 6 CONCLUSION

This study explored the effectiveness of URDA in NWP by investigating the properties of URDA in nonlinear models and proposing technical treatments to address its limitations. Specifically, it was first analytically demonstrated that, in a nonlinear model, the preemptive forecast obtained by URDA is approximately equivalent to the forecast derived from the analysis. Furthermore, this study implemented URDA based on LETKF, and numerical experiments were conducted using the Lorenz 96 model. As a result, URDA in nonlinear models showed a significant tendency for the accuracy to deteriorate and for the spread to collapse when preemptive forecasts were repeatedly updated or when the forecast lead time was extended. Additionally, we examined the role of inflation and localization, which are critical techniques in NWP, in the context of URDA. It was found that although inflation and localization remain necessary in URDA, conventional inflation techniques, such as multiplicative inflation, RTPP, and RTPS, are not suitable for URDA. Therefore, this study proposed technical treatments referred to as RTBP and RTBF. It was confirmed that applying RTBP and RTBF mitigated the difficulties of URDA in nonlinear models. Based on the insights gained from this study, we conclude that URDA, particularly when enhanced by RTBP and RTBF, offers benefits even in nonlinear models and is promising for NWP applications.

This study represents a meaningful advance toward NWP beyond Potthast and Welzbacher (2018), which used the Lorenz 63 model. However, inherent limitations remain in evaluating the effectiveness of URDA for NWP using idealized experiments with the 40-variable Lorenz 96 model. In particular, there is concern that uncertainties not addressed in the idealized experiments, such as those arising from model biases and nonlinear observation operators, may adversely affect the performance of URDA in realistic scenarios. Therefore, to further verify and refine the practical value of URDA, it is crucial to conduct URDA experiments using realistic NWP models and real observations as the next step.

## A PROPERTY OF THE ENSEMBLE TRANSFORM MATRIX

We describe some properties of the ensemble transform matrix  $\tilde{\mathbf{W}}_j^{prod}$ . First, we show that  $\tilde{\mathbf{W}}_j^{prod}$  can be decomposed into  $\mathbf{w}_j^{prod}$  and  $\mathbf{W}_j^{prod}$ .

**Proposition A.1.** *For the ensemble transform matrix  $\tilde{\mathbf{W}}_j^{prod}$ , the following equation holds:*

$$\tilde{\mathbf{W}}_j^{prod} = \frac{1}{\sqrt{m-1}} \mathbf{w}_j^{prod} \mathbf{1}^\top + \mathbf{W}_j^{prod}. \quad (49)$$

*Proof.* For  $j = 1$ , Equation (49) holds as follows:

$$\tilde{\mathbf{W}}_1^{prod} = \tilde{\mathbf{W}}_1 = \frac{1}{\sqrt{m-1}} \mathbf{w}_1 \mathbf{1}^\top + \mathbf{W}_1 = \frac{1}{\sqrt{m-1}} \mathbf{w}_1^{prod} \mathbf{1}^\top + \mathbf{W}_1^{prod}. \quad (50)$$

We assume that Equation (49) holds for  $j = t$ . Then, considering the case  $j = t + 1$ , noting that

$\mathbf{1}^\top \mathbf{w}_j = 0$  and  $\mathbf{1}^\top \mathbf{W}_j = \mathbf{1}^\top$ , the following equation holds:

$$\begin{aligned}
\widetilde{\mathbf{W}}_{t+1}^{prod} &= \widetilde{\mathbf{W}}_t^{prod} \widetilde{\mathbf{W}}_{t+1} \\
&= \left( \frac{1}{\sqrt{m-1}} \mathbf{w}_t^{prod} \mathbf{1}^\top + \mathbf{W}_t^{prod} \right) \left( \frac{1}{\sqrt{m-1}} \mathbf{w}_{t+1} \mathbf{1}^\top + \mathbf{W}_{t+1} \right) \\
&= \frac{1}{\sqrt{m-1}} \left( \mathbf{w}_t^{prod} + \mathbf{W}_t^{prod} \mathbf{w}_{t+1} \right) \mathbf{1}^\top + \mathbf{W}_t^{prod} \mathbf{W}_{t+1} \\
&= \frac{1}{\sqrt{m-1}} \mathbf{w}_{t+1}^{prod} \mathbf{1}^\top + \mathbf{W}_{t+1}^{prod}.
\end{aligned} \tag{51}$$

Therefore, because it also holds for  $j = t + 1$ , Equation (49) holds for all  $j$ .  $\square$

Subsequently, regarding the column sums of  $\widetilde{\mathbf{W}}_j^{prod}$ , the following proposition is presented.

**Proposition A.2.** *For the ensemble transform matrix  $\widetilde{\mathbf{W}}_j^{prod}$ , the following equation holds:*

$$\mathbf{1}^\top \widetilde{\mathbf{W}}_j^{prod} = \mathbf{1}^\top. \tag{52}$$

*Proof.* For the ensemble transform matrix  $\widetilde{\mathbf{W}}_j$ , noting that  $\mathbf{1}^\top \mathbf{w}_j = 0$  and  $\mathbf{1}^\top \mathbf{W}_j = \mathbf{1}^\top$ , the following equation holds:

$$\mathbf{1}^\top \widetilde{\mathbf{W}}_j = \frac{1}{\sqrt{m-1}} \mathbf{1}^\top \mathbf{w}_j \mathbf{1}^\top + \mathbf{1}^\top \mathbf{W}_j = \mathbf{1}^\top. \tag{53}$$

Therefore, we have:

$$\mathbf{1}^\top \widetilde{\mathbf{W}}_j^{prod} = \mathbf{1}^\top \widetilde{\mathbf{W}}_1 \cdots \widetilde{\mathbf{W}}_j = \mathbf{1}^\top \widetilde{\mathbf{W}}_2 \cdots \widetilde{\mathbf{W}}_j = \cdots = \mathbf{1}^\top, \tag{54}$$

because Equation (52) holds.  $\square$

Additionally, with respect to the row sums of  $\widetilde{\mathbf{W}}_j^{prod}$ , the following proposition is derived.

**Proposition A.3.** *For the ensemble transform matrix  $\widetilde{\mathbf{W}}_j^{prod}$ , the following equation holds:*

$$\widetilde{\mathbf{W}}_j^{prod} \mathbf{1} = \frac{m}{\sqrt{m-1}} \mathbf{w}_{t+1}^{prod} + \mathbf{1}. \tag{55}$$

*Proof.* From proposition A.1, noting that  $\mathbf{W}_j \mathbf{1} = \mathbf{1}$ , we have:

$$\begin{aligned}
\widetilde{\mathbf{W}}_j^{prod} \mathbf{1} &= \frac{1}{\sqrt{m-1}} \mathbf{w}_j^{prod} \mathbf{1}^\top \mathbf{1} + \mathbf{W}_j^{prod} \mathbf{1} \\
&= \frac{m}{\sqrt{m-1}} \mathbf{w}_j^{prod} + \mathbf{1}.
\end{aligned} \tag{56}$$

Therefore, Equation (55) holds.  $\square$

As shown in the following corollaries,  $\mathbf{w}_j^{prod}$  and  $\mathbf{W}_j^{prod}$  can be expressed using  $\widetilde{\mathbf{W}}_j^{prod}$ .

**Corollary A.4.** *Using the ensemble transform matrix  $\widetilde{\mathbf{W}}_j^{prod}$ , the vector  $\mathbf{w}_j^{prod}$  can be expressed as follows:*

$$\mathbf{w}_j^{prod} = \frac{\sqrt{m-1}}{m} \left( \widetilde{\mathbf{W}}_j^{prod} - \mathbf{I} \right) \mathbf{1}. \tag{57}$$

*Proof.* This follows directly from proposition A.3.  $\square$

**Corollary A.5.** *Using the ensemble transform matrix  $\widetilde{\mathbf{W}}_j^{prod}$ , the ensemble transform matrix  $\mathbf{W}_j^{prod}$  can be expressed as follows:*

$$\mathbf{W}_j^{prod} = \widetilde{\mathbf{W}}_j^{prod} - \frac{1}{m} \left( \widetilde{\mathbf{W}}_j^{prod} - \mathbf{I} \right) \mathbf{J}. \tag{58}$$

*Proof.* This follows directly from proposition A.1 and corollary A.4.  $\square$

## ACKNOWLEDGEMENTS

The authors thank Dr. Tadashi Tsuyuki of the Meteorological Research Institute for valuable discussions and insights that contributed to this study.

## FINANCIAL SUPPORT

This study was supported by the Japan Society for the Promotion of Science (JSPS) through KAKENHI (Grant Numbers 25KJ0729 and 25H00752), the Japan Science and Technology Agency (JST) Moonshot Research and Development Program (JPMJMS2389), the Institute for Advanced Academic Research (IAAR) Research Support Program, and the Virtual Laboratory (VL) Program of Chiba University.

## REFERENCES

Anderson, J. L. and Anderson, S. L. (1999). A Monte Carlo Implementation of the Nonlinear Filtering Problem to Produce Ensemble Assimilations and Forecasts. *Monthly Weather Review*, 127(12):2741–2758. Publisher: American Meteorological Society Section: Monthly Weather Review.

Bauer, P., Thorpe, A., and Brunet, G. (2015). The quiet revolution of numerical weather prediction. *Nature*, 525(7567):47–55. Publisher: Nature Publishing Group.

Bishop, C. H., Etherton, B. J., and Majumdar, S. J. (2001). Adaptive Sampling with the Ensemble Transform Kalman Filter. Part I: Theoretical Aspects. *Monthly Weather Review*, 129(3):420–436. Publisher: American Meteorological Society Section: Monthly Weather Review.

Dimet, F.-X. L. and Talagrand, O. (1986). Variational algorithms for analysis and assimilation of meteorological observations: theoretical aspects. *Tellus A*, 38A(2):97–110. \_eprint: <https://onlinelibrary.wiley.com/doi/pdf/10.1111/j.1600-0870.1986.tb00459.x>.

Etherton, B. J. (2007). Preemptive Forecasts Using an Ensemble Kalman Filter. *Monthly Weather Review*, 135(10):3484–3495. Publisher: American Meteorological Society Section: Monthly Weather Review.

Evensen, G. (1994). Sequential data assimilation with a nonlinear quasi-geostrophic model using Monte Carlo methods to forecast error statistics. *Journal of Geophysical Research: Oceans*, 99(C5):10143–10162. \_eprint: <https://onlinelibrary.wiley.com/doi/10.1029/94JC00572>.

Evensen, G., Vossepoel, F. C., and Van Leeuwen, P. J. (2022). *Data Assimilation Fundamentals: A Unified Formulation of the State and Parameter Estimation Problem*. Springer Textbooks in Earth Sciences, Geography and Environment. Springer International Publishing, Cham.

Hunt, B. R., Kostelich, E. J., and Szunyogh, I. (2007). Efficient data assimilation for spatiotemporal chaos: A local ensemble transform Kalman filter. *Physica D: Nonlinear Phenomena*, 230(1):112–126.

Kalnay, E. (2002). *Atmospheric Modeling, Data Assimilation and Predictability*. ISBN: 9780511802270 Publisher: Cambridge University Press.

Kotsuki, S., Pensoneault, A., Okazaki, A., and Miyoshi, T. (2020). Weight structure of the Local Ensemble Transform Kalman Filter: A case with an intermediate atmospheric general circulation model. *Quarterly Journal of the Royal Meteorological Society*, 146(732):3399–3415. \_eprint: <https://rmets.onlinelibrary.wiley.com/doi/pdf/10.1002/qj.3852>.

Liu, C., Xiao, Q., and Wang, B. (2008). An Ensemble-Based Four-Dimensional Variational Data Assimilation Scheme. Part I: Technical Formulation and Preliminary Test. *Monthly Weather Review*, 136(9):3363–3373. Publisher: American Meteorological Society Section: Monthly Weather Review.

Lorenz, E. N. (1963). Deterministic Nonperiodic Flow. *Journal of the Atmospheric Sciences*, 20(2):130–141. Publisher: American Meteorological Society Section: Journal of the Atmospheric Sciences.

Lorenz, E. N. (1996). Predictability: a problem partly solved. *Seminar on Predictability, 4-8 September 1995*, 1:1–18.

Lorenz, E. N. and Emanuel, K. A. (1998). Optimal Sites for Supplementary Weather Observations: Simulation with a Small Model. *Journal of the Atmospheric Sciences*, 55(3):399–414. Publisher: American Meteorological Society Section: Journal of the Atmospheric Sciences.

Madaus, L. E. and Hakim, G. J. (2015). Rapid, short-term ensemble forecast adjustment through offline

data assimilation. *Quarterly Journal of the Royal Meteorological Society*, 141(692):2630–2642. \_eprint: <https://onlinelibrary.wiley.com/doi/pdf/10.1002/qj.2549>.

Miyoshi, T. and Aranami, K. (2006). Applying a Four-dimensional Local Ensemble Transform Kalman Filter (4D-LETKF) to the JMA Nonhydrostatic Model (NHM). *Sola*, 2:128–131.

Miyoshi, T. and Yamane, S. (2007). Local Ensemble Transform Kalman Filtering with an AGCM at a T159/L48 Resolution. *Monthly Weather Review*, 135(11):3841–3861. Publisher: American Meteorological Society Section: Monthly Weather Review.

Potthast, R. and Welzbacher, C. A. (2018). Ultra Rapid Data Assimilation Based on Ensemble Filters. *Frontiers in Applied Mathematics and Statistics*, 4. Publisher: Frontiers.

Szunyogh, I., , Eric J., K., , Gyorgyi, G., , Eugenia, K., , Brian R., H., , Edward, O., , Elizabeth, S., , and Yorke, J. A. (2008). A local ensemble transform Kalman filter data assimilation system for the NCEP global model. *Tellus A: Dynamic Meteorology and Oceanography*, 60(1):113–130. Publisher: Taylor & Francis \_eprint: <https://doi.org/10.1111/j.1600-0870.2007.00274.x>.

Talagrand, O. and Courtier, P. (1987). Variational Assimilation of Meteorological Observations With the Adjoint Vorticity Equation. I: Theory. *Quarterly Journal of the Royal Meteorological Society*, 113(478):1311–1328. \_eprint: <https://onlinelibrary.wiley.com/doi/pdf/10.1002/qj.49711347812>.

Whitaker, J. S. and Hamill, T. M. (2002). Ensemble Data Assimilation without Perturbed Observations. *Monthly Weather Review*, 130(7):1913–1924. Publisher: American Meteorological Society Section: Monthly Weather Review.

Whitaker, J. S. and Hamill, T. M. (2012). Evaluating Methods to Account for System Errors in Ensemble Data Assimilation. *Monthly Weather Review*, 140(9):3078–3089. Publisher: American Meteorological Society Section: Monthly Weather Review.

Zhang, F., Snyder, C., and Sun, J. (2004). Impacts of Initial Estimate and Observation Availability on Convective-Scale Data Assimilation with an Ensemble Kalman Filter. *Monthly Weather Review*, 132(5):1238–1253. Publisher: American Meteorological Society Section: Monthly Weather Review.

Zhang, Y., Long, M., Chen, K., Xing, L., Jin, R., Jordan, M. I., and Wang, J. (2023). Skilful nowcasting of extreme precipitation with NowcastNet. *Nature*, 619(7970):526–532. Publisher: Nature Publishing Group.